Chapter 3

Hsp70 Acts as a Guardian of Cell Survival By Inhibiting Multiple Cell Death Pathways

3.1 Abstract

Hsp70 is a multi-functional chaperone that has been implicated in numerous cancers and as a target for several therapies. However, this target has proven difficult to inhibit with small molecules. In the previous chapter, we described JG-98, a novel allosteric Hsp70 modulator. JG-98 displayed significant activity against a panel of cancer cell lines (EC_{50} ~ 400 nM) and favorable pharmacokinetics in mice. In this Chapter, we use JG-98 as a new chemical tool compound to explore the roles of Hsp70 in cancer cell survival. We report that JG-98 triggers apoptosis in a Bcl-2 independent and RIP1-kinase dependent fashion. Further, under conditions in which apoptosis is blocked, JG-98 retained its cytotoxic activity, exploiting RIP1's unique capability to facilitate programmed necrosis (necroptosis). The ability of JG-98 to induce non-apoptotic cell death has important implications for chemotherapeutic drug development. Moreover, these results also suggest that the roles of Hsp70 in cancer are distinct from those of Hsp90, as this chaperone is linked to multiple cell death pathways.

3.2 Introduction

To aid in the survival of numerous cytotoxic signals, most cancers express elevated levels of molecular chaperones, including heat shock proteins 70 (Hsp70) and 90 (Hsp90) (*1*–*6*). Both chaperones cooperate to stabilize several oncogenic "clients", provide resistance to cell death, and protect against radiation and chemotherapy (*7*–*9*). These pro-survival activities make Hsp70 and Hsp90 promising nodes for potential anti-cancer therapies. Hsp90 is the more well-studied chaperone and has been shown to govern a large subset of the proteome devoted to oncogenic activity, including kinases and transcription factors (*7*, *10*–*12*). Indeed, Hsp90 is so centrally positioned amongst these oncogenic effectors that it has been called the "Cancer Chaperone" (*13*–*15*). Further, a substantial number of small molecules have been developed to inhibit Hsp90 (*16*), and these compounds display potent efficacy in several cancer models. Yet, despite their pre-clinical successes, many of these inhibitors have struggled in clinical trials. Patients often respond quite well initially, only to relapse a short time later (*17*–*20*). Their tumors grow back, and resume resistance to the chemotherapeutics and radiation therapy originally sensitized by Hsp90 inhibition (*21*, *22*). Although the direct mechanisms for this restored oncogenic activity and resistance are unclear, the induction of Hsp70 expression upon treatment with these compounds is thought to play a vital role (*20*, *23*, *24*).

Indeed, Hsp70 itself has been shown to be upregulated in a large number of cancers and to correlate with disease progression and resistance to traditional first-line therapies (*8*, *25*–*27*). Moreover, studies have shown that knockdown of Hsp70 greatly enhances the efficacy of Hsp90 inhibitors (*28*). While the clients of Hsp90 are well

known (see above) and it is apparent that Hsp90 inhibitors induce apoptosis (*7*, *10*, *11*), the exact mechanisms by which Hsp70 protects against cell death remain unclear. Although many reports have suggested that Hsp70 regulates Hsp90 clients (*28*–*30*) and that it shares the ability of Hsp90 to inhibit both the extrinsic and intrinsic pathways of apoptosis (*31*), it is uncertain if Hsp70 is restricted to only these activities. Studies to clarify Hsp70's oncogenic activity have been limited, in part, by the lack of successful Hsp70-targeting small molecules. In the previous Chapter, we discussed the synthesis and preliminary characterization of JG-98, a novel allosteric modulator of Hsp70 and derivative of the rhodocyanine MKT-077 (*32*). JG-98 "trapped" Hsp70 in an ADP-bound state with a low affinity for nucleotide exchange factor (NEF) co-chaperones and increased substrate binding. JG-98 also displayed potent activity against multiple cancer cell lines and it had improved metabolic stability *in vivo.* In this Chapter, we further analyze JG-98's cytotoxic activities and describe its synergistic activity with Hsp90 and proteasomal inhibitors. Using JG-98, we made the unexpected discovery that Hsp70 blocks multiple cell death pathways through the cell-death switch RIP1 kinase, suggesting Hsp70's involvement in proteostasis is broader than previously known.

3.3 Results

3.3.1 JG-98 Triggers Degradation of Classical Hsp90-Clients and Induces Apoptotic Cell Death

In the previous chapter, we showed that JG-98 stabilized Hsp70 in an ADP-bound conformation, with a low affinity for Bag3 co-chaperone, and high affinity for protein substrates. Interrupting Hsp70's chaperone cycle appears to target chaperone clients for degradation, including Akt, Raf-1, and Cdk4 kinases (Figure 3.1.A), similar to what is observed after treatment with 17-DMAG, an Hsp90 inhibitor, or bortezomib. However, unlike Hsp90 or proteasome inhibition, JG-98 did not induce a stress response in MDA-MB-231 cells (Figure 3.1.A), as shown by the constant levels of Hsp70. The lack of a stress response by JG-98 is consistent with previous work from our group, showing that Hsp70 inhibitors with a variety of mechanism do not promote a stress response (*33*, *34*).

We observed caspase-3 and PARP cleavage upon JG-98 treatment, and thus investigated whether these molecular changes were reflective of an apoptotic cascade. Microscopy revealed apoptotic-like features such as cell shrinkage, rounding, and membrane blebbing (Figure 3.1.B) after 24 hours. Further, Hoechst staining revealed DNA-fragmentation and 80% of the cells treated with JG-98 became double positive for the apoptotic markers annexinV+ and DAPI- after 48 hours (Appendix 3.1). Together, this data suggest that JG-98 triggers degradation of classical Hsp90-clients and induces a classic caspase-dependent apoptotic cascade.

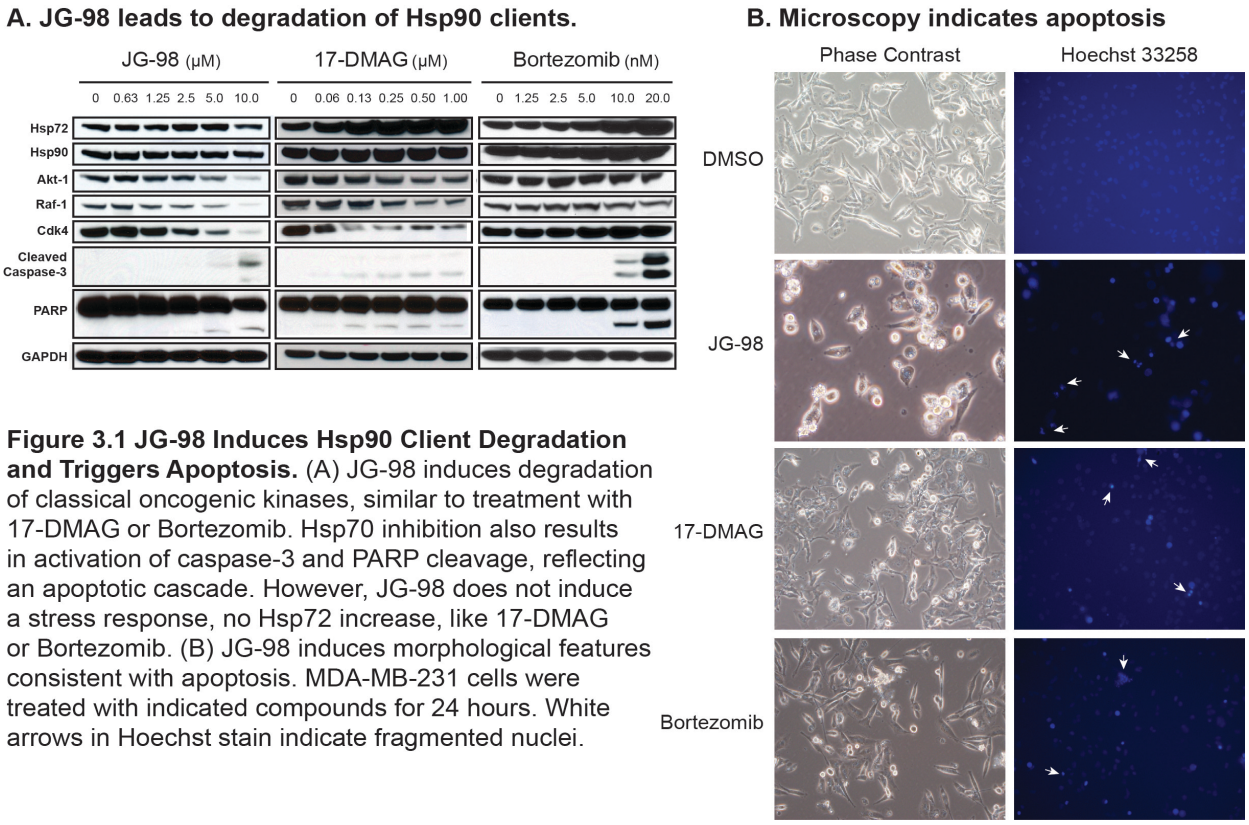

Figure 3.1 JG-98 Induces Hsp90 Client Degradation and Triggers Apoptosis. (A) JG-98 induces degradation of classical oncogenic kinases, similar to treatment with 17-DMAG or Bortezomib. Hsp70 inhibition also results in activation of caspase-3 and PARP cleavage, reflecting an apoptotic cascade. However, JG-98 does not induce a stress response, no Hsp72 increase, like 17-DMAG or Bortezomib. (B) JG-98 induces morphological features consistent with apoptosis. MDA-MB-231 cells were treated with indicated compounds for 24 hours. White arrows in Hoechst stain indicate fragmented nuclei.

3.3.2 Targeting Hsp70 is Highly Synergistic with Hsp90 or Proteasomal Inhibition

Due to their apparent cooperative activities in governing the oncogenic proteome, it has been suggested that combinatorial therapy targeting both Hsp70 and Hsp90 or the proteasome would be highly synergistic. Powers *et al.* showed that knockdowns of both Hsc70 and Hsp72 potentiated treatment with the Hsp90 inhibitor 17-AAG (*28*). Other studies have also shown synergy between small molecule inhibitors of Hsp70 and Hsp90 (*29*, *35*). However, these studies have been limited by the lack of potent compounds targeting Hsp70. Additionally, the mechanism of synergy for these combinations has not been fully characterized.

Before moving on, it is worthwhile to note that the term “synergistic” is often mistakenly used to describe compounds that are merely “additive.” Particularly with regards to chemotherapeutics, adding one cytotoxic agent to another will usually result in increased cell death. However, the true definition of synergy is actually *quantitative* (*36*), and can only be measured by calculating the Combination Index (CI), a readout of the ratio between the most potent combination doses (e.g. Two drugs at doses C_X and C_Y) and the individual IC values for those drugs (e.g. IC_X and IC_Y). Thus, the CI value for any desired effect (in this case, percent cell death) can be calculated as:

$$CI(\%) = [\frac{C_X}{IC(\%)_X}] + [\frac{C_Y}{IC(\%)_Y}]$$

Values less than 1 indicate synergy, while greater than 1 suggests an antagonistic nature. A CI value equal to 1 defines a simple additive effect.

To understand the true effect of targeting both Hsp70 and Hsp90 or the proteasome, we combined JG-98 with 17-DMAG or bortezomib and measured the viability of MDA-MB-231 cells (Figures 3.2.A and 3.2.D). Both JG-98/17-DMAG and JG-98/bortezomib combinations exhibit very strong synergism with decreasing CI values at increased cell death (CI_{95} values < 0.2) (Figures 3.2.B and 3.2.E). The exact mechanism for this improved synergy at more cytotoxic dosing is unclear, but a potential explanation is provided here. We have previously commented that both 17-DMAG and bortezomib suffer from resistance through Hsp70 induction, and that this stress response occurs in a dose-dependent manner. Thus, it is reasonable to suggest that the addition of an Hsp70 inhibitor, such as JG-98, would be most synergistic when the stress response phenotype is peaked - in this case, at higher doses. Interestingly, JG-98/bortezomib, when given at 1:1 ratios, did not display this trend. In this case, the

higher content of bortezomib in that particular dose ratio likely triggers a stress response at lower cytotoxic values, thus facilitating strong synergy at all CI ratios.

To further characterize the synergy between members of the PQC machinery, we examined whether the combinations of compounds would have an effect on the stability of chaperone clients. We found that combinations of JG-98 with 17-DMAG or bortezomib caused dramatically improved degradation of Akt, Raf-1, and Cdk4. These clients were degraded at significantly lower concentrations when used in concert (Figures 3.2.C and 3.2.F). The combinations of 17-DMAG and bortezomib with JG-98 induced a stress response when the two compounds were added simultaneously. However, pre-treatment of cells with JG-98 for 4 hours blocked the stress response induced by 17-DMAG (Neckers unpublished/personal communication).

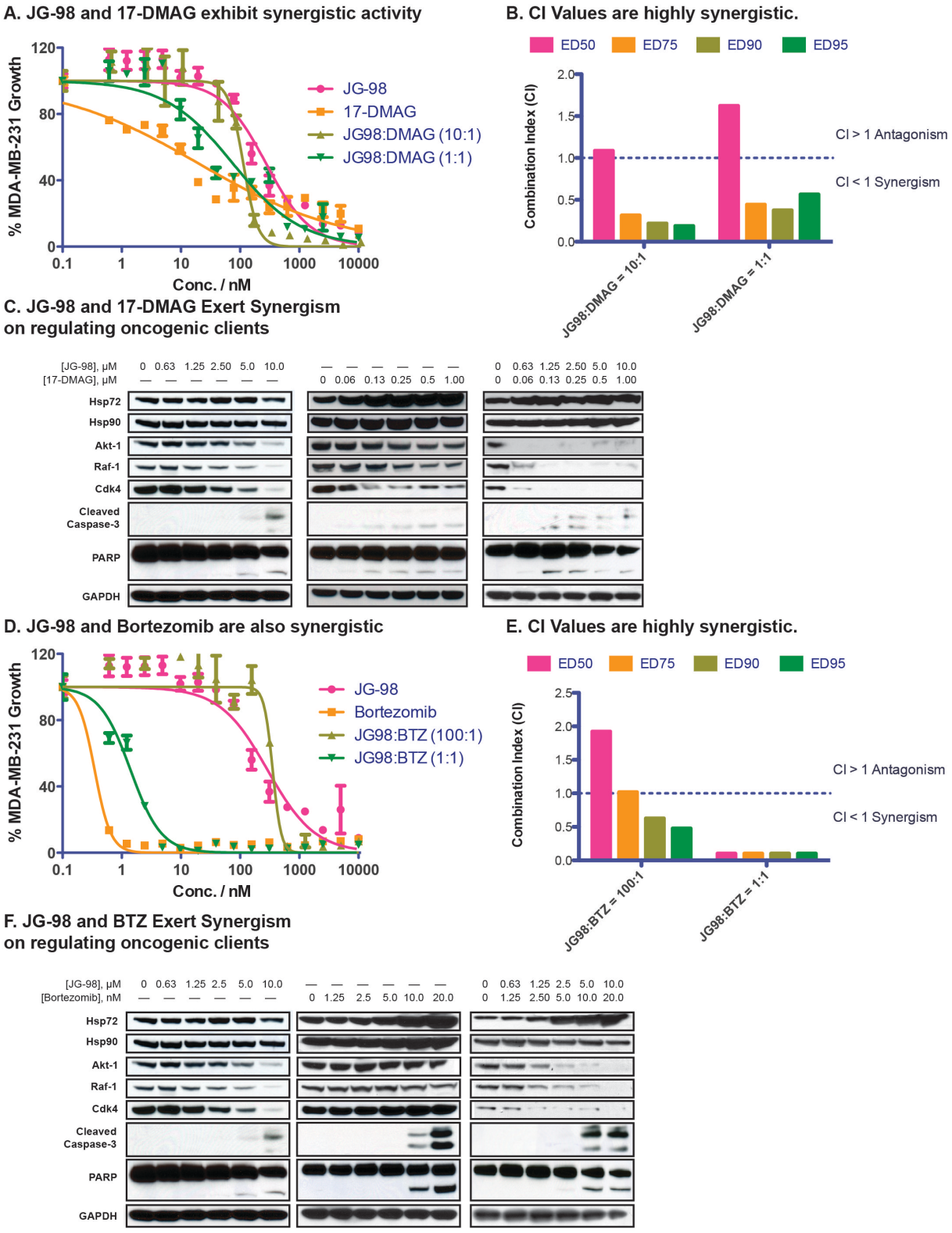

Figure 3.2 JG-98 is Synergistic with Inhibitors of PQC Machinery. JG-98 exhibits synergistic anti-cancer activity with 17-DMAG (A) and Bortezomib (D). Synergy is quantified using combination indices (B) and (E). Oncogenic clients Akt, Raf-1, and Cdk4 are degraded with increased efficacy in response to combination treatments (C) and (F).

3.3.3 JG-98 Induces a Rapid Cell Death

Thus far, the results seemed to indicate that Hsp70 and Hsp90 have similar and largely redundant roles in protecting chaperone clients and inhibiting apoptosis. However, we noted that the effect of JG-98 on the chaperone clients (when used as a single agent) were relatively modest. Moreover, cell death in response to JG-98 treatment was rapid when compared to Hsp90 or proteasome inhibition (Figure 3.3.A). The kinetics of cell death did not coincide with loss of Akt, Raf-1 or Cdk4, which were only lost hours after the initiation of cell death in the MDA-MB-231 cells (Figure 3.3.B). A striking feature of Hsp90 inhibitors is that the loss of clients occurs at the same time as the initiation of cell death (*37*, *38*). These observations were our first indication that there was a substantial difference in the way that Hsp70 and Hsp90 were protecting the cells from cell death.

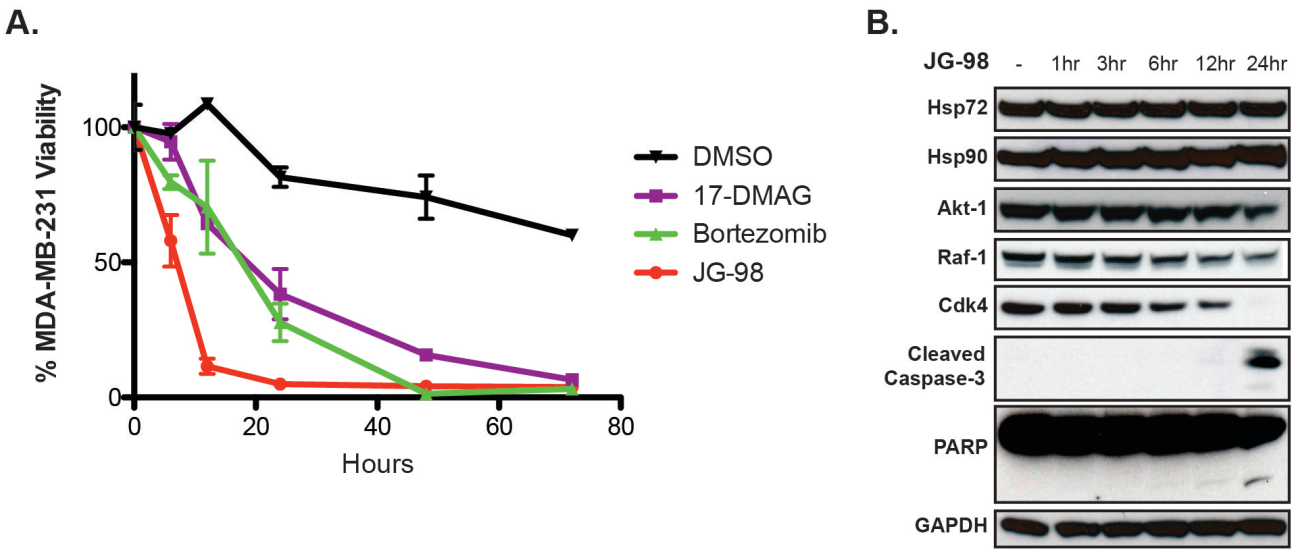

Figure 3.3 Hsp70 Inhibition Elicits Rapid Cell Death. (A) JG-98 Triggers loss of cell viability significantly faster than Hsp90 or proteasomal inhibition. (B) Degradation of Hsp90 clients by JG-98 lags behind cell death, suggesting alternative death pathways.

3.3.5 JG-98's Cytotoxicity Proceeds Independently of the Mitochondria

To further understand the apoptotic cascade triggered by JG-98, we genetically overexpressed the Bcl-2 family member, Bcl-xL in MDA-MB-231 and Jurkat cells using a lentiviral system. Overexpression of Bcl-xL blocked the cytotoxicity of 17-DMAG and bortezomib, as expected, but it did not impede JG-98 cytotoxicity (Figures 3.4.A and B). Microscopic examination revealed that JG-98 treatment still induced features consistent with apoptosis, similar to cells transduced with lentiviral vector only (Figure 3.4.C). Control transduced cells showed cytosolic release of both cytochrome c and Smac/DIABLO, suggesting that JG-98 engages the mitochondrial death pathway en route to apoptosis (Figure 3.4.D). However, Bcl-xL overexpression only suppressed relocalization of Smac, while JG-98 still triggered release of cytochrome c. The ability of JG-98 to induce cytochrome c release even in the presence of high Bcl-xL levels likely results from its actions on mitochondrial Hsp70 (see Chapter 2: Conclusions). The exact mechanism for this selective effect on cytochrome c will be the subject of future studies, but the result has enormous implications for treatments of several cancers where Bcl-2 overexpression is a driving mutation, such as in follicular lymphoma (*39*).

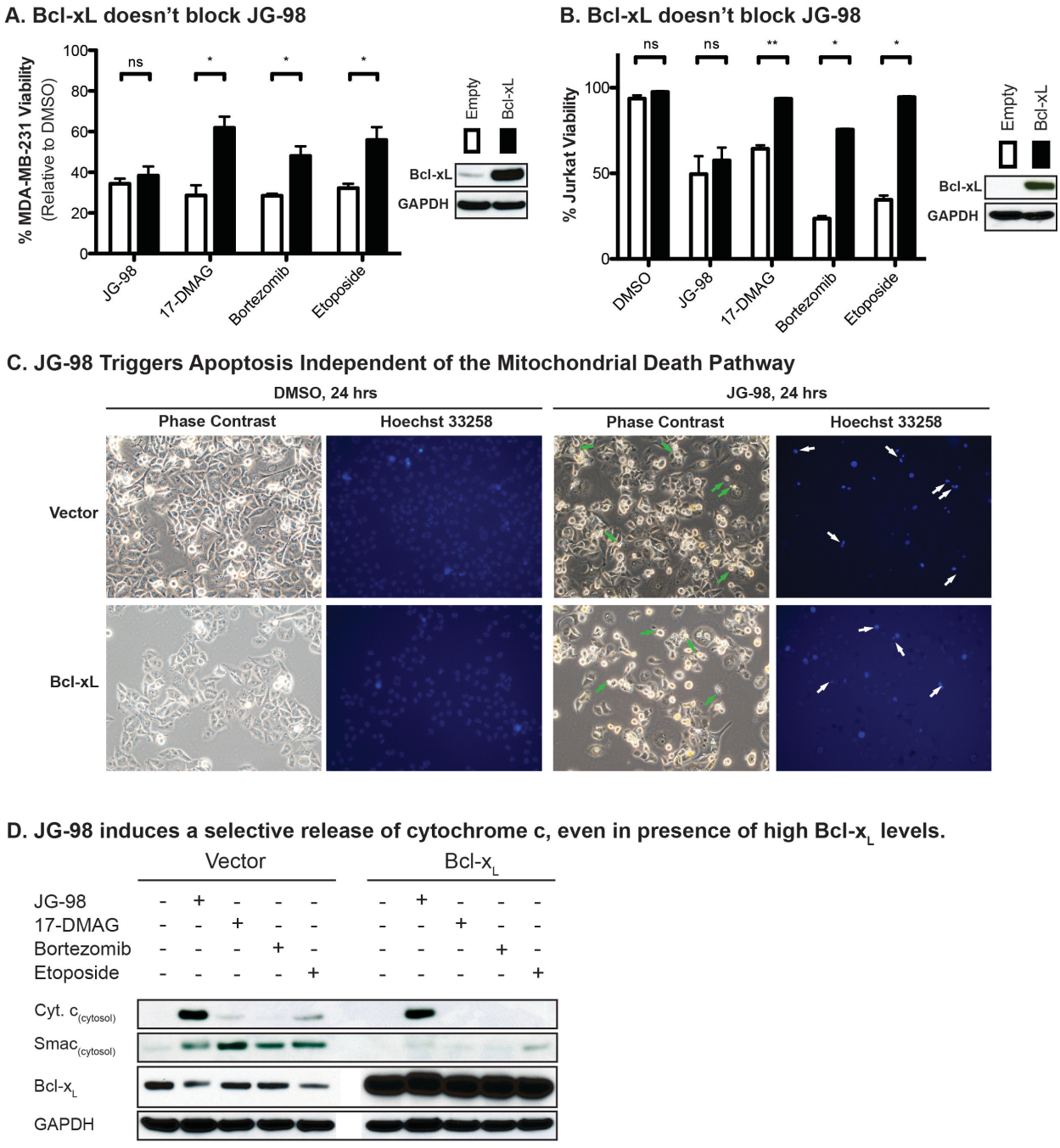

Figure 3.4 JG-98 Induces Cell Death Independent of Bcl-2 Status. MDA-MB-231 (A) and Jurkat (B) cells overexpressing Bcl-xL are equally sensitive as wild-type to JG-98 treatment. Viability determined by MTT assay (A) and Trypan Blue Exclusion (B). (C) Microscopy of MDA-MB-231 cells show that JG-98 treatment still induces apoptosis in Bcl-xL cells. (D) JG-98 induces cytoplasmic release of cytochrome c and Smac, but Bcl-xL expression only suppresses Smac release. Extracts made using digitonin treatment and verified by blotting for CoxIV (not shown).

3.3.5 Caspase Inhibition Alters JG-98 Cytotoxic Phenotype

Despite circumventing Bcl-2 inhibition, JG-98's cytotoxic effects appear to trigger caspase-3 cleavage and thus, should be recovered by blocking caspase activity. To this end, we pre-treated MDA-MB-231 and Jurkat cells with z-VAD.fmk, a pan-caspase inhibitor. Although it recovered viability for cells treated with 17-DMAG or bortezomib (Figure 3.5.A and Appendix 3.2), z-VAD.fmk did not block JG-98 cytotoxicity. We examined the treated cells by fluorescent microscopy and observed that pre-treatment with z-VAD.fmk prior to JG-98 yielded cells with swollen cytoplasm and intracellular granules (Figure 3.5.B). These morphological features are consistent with necrosis instead of apoptosis. As further evidence of this alternative cell death pathway, we observed no nuclear fragmentation in z-VAD pre-treatments by Hoechst stain.

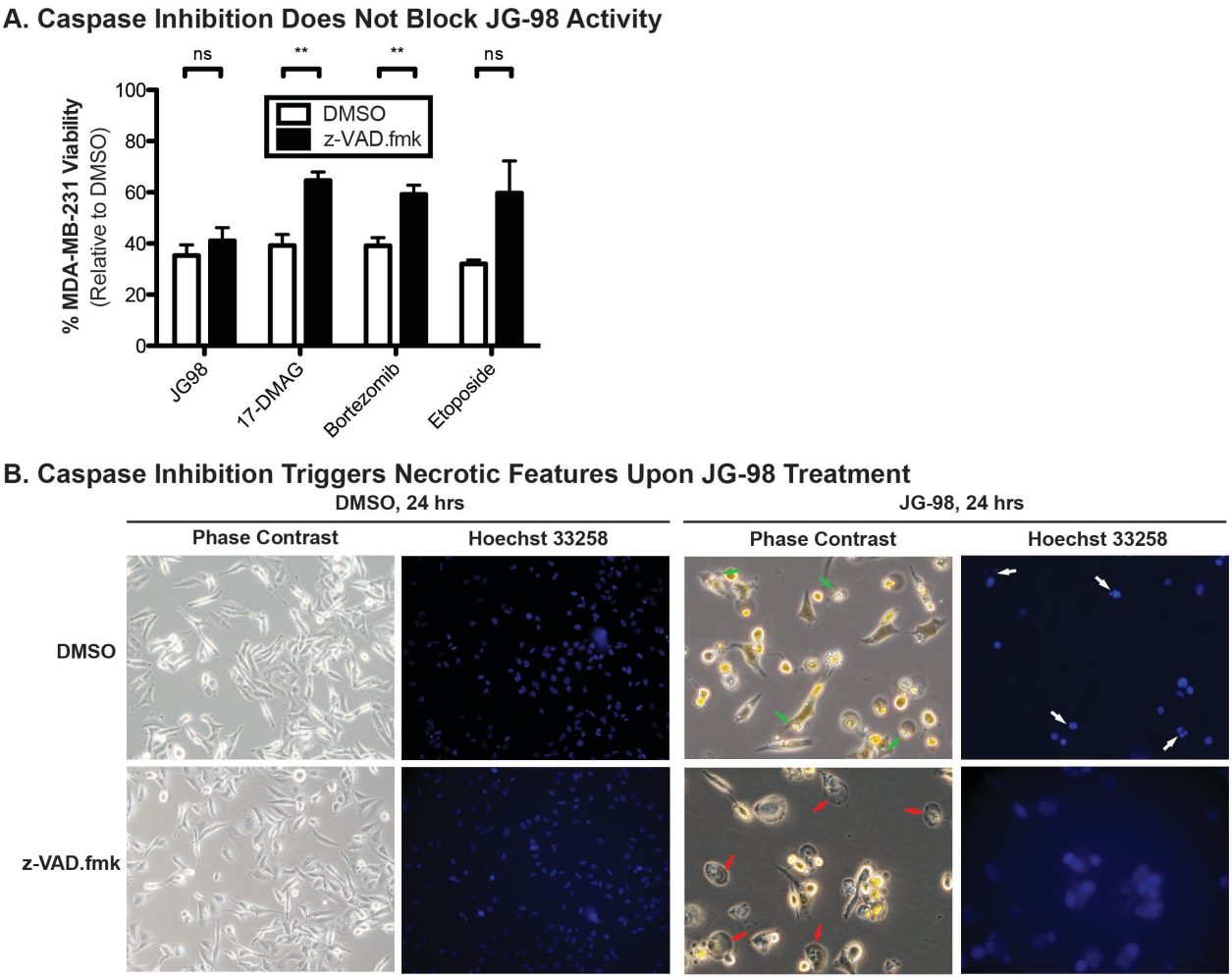

Figure 3.5 Caspase Inhibition Switches Cell Death Morphology. (A) Pretreatment of MDA-MB-231 cells with a caspase inhibitro, z-VAD.fmk, does not block JG-98 induced cell death. Viability determined by MTT assay. (B) Microscopy reveals that caspase-inhibition switches cell death morphology by JG-98. Arrow markings, green: apoptotic cells, red: necrotic cells, white: fragmented nuclei.

3.3.6 Cytotoxic Effects of JG-98 Depend on RIP1-Kinase

RIP1 is a kinase that directs cells into either the apoptotic or necroptotic (programmed necrosis) cascades (*40–42*). Because JG-98 appeared to be directing cells into both pathways, we explored whether Hsp70 might be involved in RIP1 regulation. We first explored RIP1$^{-/-}$ Jurkat cells and found they were resistant to JG-98 treatment (Figure 3.6.A). Similarly, treatment with the small molecule Necrostatin-1

(Nec-1), a recently discovered inhibitor of RIP1's kinase activity (*43*), also blocked JG-98 cytotoxicity. Nec-1 is also capable of blocking necroptosis under conditions where apoptosis has already been inactivated (*44*). Consistent with this activity, cells pre-treated with Nec-1 were nearly completely resistant to treatment with JG-98 (Figure 3.6.B and Appendix 3.2). Together these data suggest JG-98's cytotoxicity is dependent on RIP1, and specifically its kinase activity.

We then examined JG-98's direct effects on RIP1 and its modulators. It has recently been identified that RIP1 is constitutively ubiquitinated by the E3 ligases XIAP, c-IAP1, c-IAP2, and cFLIP (*45*). JG-98 treatment induced dose-dependent degradation of all these negative modifiers (Figure 3.6.C). However, RIP1 levels were unaffected, suggesting one of two mechanisms: 1) JG-98 does not lead to RIP1 stabilization but merely prevents basal RIP1 degradation; or 2) JG-98 frees a separate pool of RIP1 that is normally degraded and is capable of triggering cell death.

To test if the role of Hsp70 in RIP1 regulation was more directly related to cell death, we measured how fast RIP1 modulators were degraded in response to JG-98. Unlike what we observed with the loss of Akt and other classic clients, we found that the kinetics of RIP1 modulator degradation more closely paralleled cytotoxicity (Figure 3.6.D). In addition, we noticed that the loss of Inhibitor of Apoptosis Proteins (IAPs) was less pronounced than the degradation of both isoforms of cFLIP. Thus, stabilization of cFLIP might be an especially important role for Hsp70.

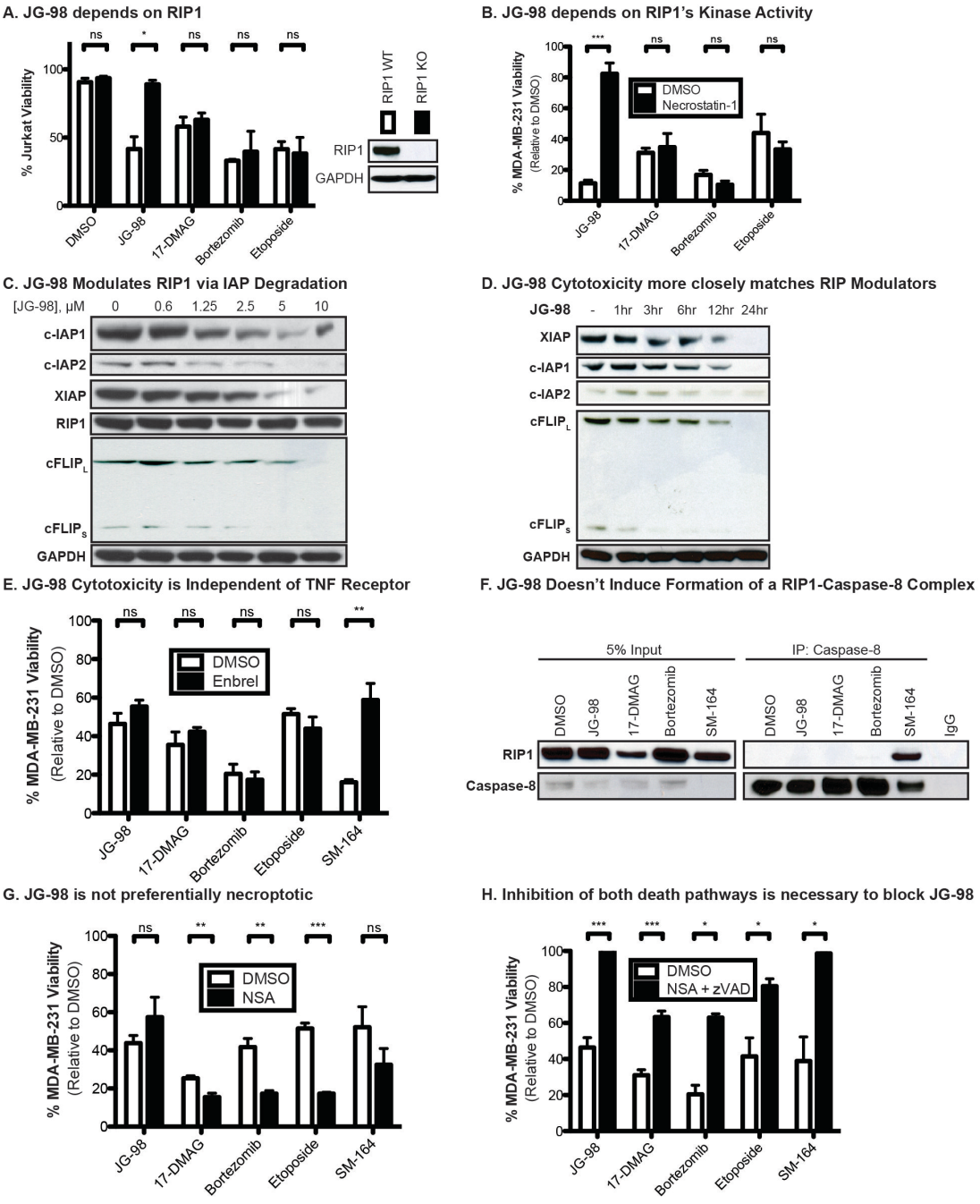

Figure 3.6 JG-98 Induces Cell Death Through a Novel RIP1-Dependent Process. (A) RIP1 $^{-/-}$ cells are resistant to JG-98. Viability was determined by Trypan Blue Exclusion. **(B)** JG-98 cytotoxicity requires RIP1's kinase activity. Cells were pretreated with 20μM Necrostatin-1 for 1 hour prior to addition of compounds. Viability was determined by MTT assay. **(C)** JG-98 induces degradation of RIP1 modulators, but does not affect RIP1 levels. MDA-MB-231 cells were treated for 24 hours with JG-98 at indicated doses. **(D)** RIP1 ubiquitinators are rapidly degraded in response to JG-98. MDA-MB-231 cells were treated with 10μM JG-98 for indicated time periods. **(E)** JG-98 toxicity does not depend on TNF signaling. Cells were pretreated with 5ug/ml Enbrel for 1 hour prior to addition of compounds. Viability was determined by MTT assay. **(F)** JG-98 does not induce formation of a RIP1-Caspase-8 complex (Ripoptosome). MDA-MB-231 cells were pretreated with z-VAD for 1 hour and then 24 hours with indicated compounds. Caspase-8 was immunoprecipitated as previously described (Tenev. et al) and RIP1 interaction was probed by western blot. **(G)** JG-98 does not preferentially activate necroptosis. Cells were pretreated with 20μM Necrosulfonamide (NSA) for 1 hour prior to addition of compounds. **(H)** Inhibition of both apoptosis and necroptosis is necessary to recover from JG-98 cytotoxicity. Cells were pretreated with both 20μM z-VAD.fmk and 20μM NSA for 1 hour prior to addition of compounds. Viability was determined by MTT assay.

3.3.7 JG-98 Activates a Novel RIP1-Dependent Death Pathway

We then investigated the cellular processes involving RIP1 that might be triggered by JG-98. One major role for RIP1 is as a central scaffold in TNF-Receptor I, a complex capable of mediating both apoptosis and necroptosis (*40*). Recently, it has been shown that autocrine-TNF-producing cells, such as MDA-MB-231, are sensitive to small molecule mimetics of Smac/DIABLO (*41*), and that this cytotoxicity proceeds through TNF-R1. We investigated this possibility, and found that an antibody against TNF-R1 (Enbrel) was unable to prevent JG-98 mediated cell death, though it significantly recovered treatment with a smac-mimetic SM-164 (Figure 3.6.E). Further, JG-98 showed no activation of the NF-κB pathway (Andy Kocab, Duckett Lab, Michigan). These results are consistent with Hsp70 serving a role in regulating RIP1 independent of TNF-R1.

Recently, a novel cytosolic death complex, the “Ripoptosome”, has been described to consist of RIP1, caspase-8, and FADD (*41*). The Ripoptosome was shown to be a unique species from TNF-R1 Complex II, though the constituents were largely the same. Like TNF-R1 Complex II, the Ripoptosome is negatively regulated by the IAPs and $cFLIP_L$. To determine if JG-98 triggered formation of the Ripoptosome, we immunoprecipitated Caspase-8 and blotted for RIP1 interaction. As expected, SM-164 induced a strong association between caspase-8 and RIP1; however, this interaction was not promoted by JG-98 (Figure 3.6.F). Thus, the RIP1-mediated cell death induced by JG-98 appears to proceed through a new mechanism.

3.3.8 Blockade of both Apoptosis and Necroptosis is Necessary to Inhibit JG-98 Cytotoxicity

Next, we wondered whether blocking necroptosis would be sufficient to inhibit cytotoxicity in response to JG-98. To test this idea, we employed the necroptosis-specific inhibitor, Necrosulfonamide (NSA) (*46*). Pretreatment of MDA-MB-231 or Jurkat cells did not protect against JG-98 cytotoxicity (Figure 3.6.G and Appendix 3.2). However, the combination of z-VAD.fmk and NSA *was* sufficient to block JG-98 (Figure 3.6.H and Appendix 3.2), suggesting that inactivation of *both* apoptotic and necroptotic pathways are required to recover cell viability. This data recapitulates the effects of inhibiting RIP1's kinase activity genetically (Figure 3.6.A) or chemically (Figure 3.6.B), effectively severing the upstream signal for both apoptosis and necroptosis.

3.4 Discussion

Due to their dependence on metastable oncogenic proteins for viability and proliferation, cancer cells have been described as "addicted" to molecular chaperones (*13*, *47*, *48*). To this end, Hsp90, as a central regulator of many oncogenic proteins and inhibitor of apoptosis, has been the target of numerous anti-cancer drug campaigns (*16*). However, these efforts have suffered from developed tolerance and resistance, often driven by induction of Hsp90's sister chaperone, Hsp70. Itself a potent inhibitor of apoptosis, Hsp70 has emerged as the subject of newer studies on proteostatic regulation of cancer cells (*49*, *50*). While Hsp90's clientele has been well defined (*7*, *10*–*12*), the analogous pool for Hsp70 is not known. Studies have shown that Hsp70

does indeed have the ability to regulate the stability of Hsp90 clients (*28*–*30*), but it is unclear if Hsp70's oncogenic activities are restricted to the Hsp90 pool.

In Chapter 2, we described a novel allosteric inhibitor of Hsp70, JG-98, with anti-cancer activity (*32*). In this chapter, we further characterized JG-98's cytotoxic nature. We found that JG-98 treatment led to the degradation of oncogenic clients, such as Akt, Raf-1, and Cdk4, which are also known to be regulated by Hsp90. Thus, Hsp70 does share some responsibilities with Hsp90 in cancer cells. However, we also noticed some significant and interesting differences. Specifically, we noted that the degradation of the classical clients occurred with kinetics that did not correlate with the progression of cytotoxicity; JG-98 triggered cell death much faster than 17-DMAG or bortezomib.

Before discussing the major differences between the functions of Hsp70 and Hsp90 in cancer signaling, it is worth pointing out that inhibition of Hsp70 did not activate a stress response. Inhibitors of either Hsp90 or the proteasome activate a cellular stress response and elevate the levels of other chaperones and components of the protein quality control system, including Hsp70. The increase in these proteins is believed to be a major driving force in chemotherapeutic resistance. Thus, it has been hypothesized that the combination of these drugs with an Hsp70 inhibitor might be highly desirable. Indeed, we found that JG-98 has highly synergistic activity with both 17-DMAG and bortezomib, especially at more lethal doses, where Hsp70 induction is highest. We also observed greatly increased degradation of client proteins at dosing well below that for any individual compound. It is not known why inhibition of Hsp70 by JG-98 (or other inhibitors) does not activate a stress response. Hsp70 is known to

interact with the major heat shock transcription factor (HSF1), yet JG-98 did not activate HSF1 activity, suggesting that Hsp70 is not required to block HSF1 function.

One of the major goals of this thesis work was to better understand the roles of Hsp70 in cancer signaling. Using JG-98 as a tool, we now had the opportunity to address this important question. Although inhibition of Hsp70 compared with Hsp90 and proteasome inhibition in the ability to induce apoptotic cell death, we found that overexpression of the anti-apoptotic Bcl-2 member, Bcl-xL, was not enough to recover cell viability. Bcl-xL overexpressing cells were not resistant to JG-98, still displaying morphological features associated with apoptosis and maintaining cytosolic release of cytochrome c, but not Smac. Thus, Hsp70 appears to suppress the mitochondrial death pathway independent of the status of Bcl-2 family members. It is not yet clear why Smac is not released in the Bcl-xL overexpressing cells treated with JG-98. However, Hsp70 inhibition seems to enact a redundancy in Smac function by directly regulating the stability of the IAPs, permitting the apoptotic pathway even in the absence of Smac release. Regardless, the cytotoxicity of JG-98 in the presence of high Bcl-xL is an important finding because it suggests that inhibition of Hsp70 will still be effective in cancers with high Bcl-2 expression.

When Hsp70 is inhibited, caspase-3 and PARP are cleaved; however, inhibition of caspase activity by z-VAD.fmk did not diminish JG-98 cytotoxicity. Instead, we observed dramatic changes in cellular morphology, including cytoplasmic swelling and intracellular granules, more consistent with necrosis. This was an unexpected result, as Hsp70 had extensively been linked to the apoptosis pathways, but not to necrosis. To explore this mechanism in greater detail, we studied the possible relationship between

Hsp70 and RIP1. RIP1 kinase has been implicated as a regulator of apoptosis and necroptosis, or programmed necrotic cell death (*40*–*42*). RIP1$^{-/-}$ Jurkat cells were resistant to the Hsp70 inhibitor, as were those pre-treated with Necrostatin-1, a chemical inhibitor of RIP1's kinase activity. Moreover, JG-98 induced the degradation of known negative regulators of RIP1, including the IAPs and cFLIP. Thus, our data is consistent with a model in which cell death induced by JG-98 proceeds through the "fork" of RIP1 kinase (Figure 3.7), likely by triggering the degradation of its negative regulators. Given the option of two cytotoxic paths, cells will undergo apoptosis after Hsp70 inhibition. However, under situations in which apoptosis has been inactivated, such as with a caspase-inhibitor or genetic alteration, cells may still die through necroptosis. Indeed, downstream of RIP1, a blockade of both apoptotic and necroptotic cascades was necessary to block JG-98 cytotoxicity. Further, JG-98 activity was found to be independent of TNF-Receptor function, again suggesting that Hsp70 operates autonomous of receptor signaling. In addition, JG-98 did not trigger a Caspase-8-RIP1 interaction (*41*, *45*), suggesting that it operates by a different RIP1 dependent mechanism than previously known.

The ability of JG-98 to trigger necroptosis has important implications for future chemotherapeutic regimens targeting the protein quality control machinery. Given its highly synergistic activity, the combination of either 17-DMAG or Bortezomib with an Hsp70 inhibitor is likely to exhibit clinical successes where the individual compounds failed. Whether this synergy is due to doubly inducing the same apoptotic pathway, or by simultaneously triggering both apoptotic and necroptotic events will need to be explored.

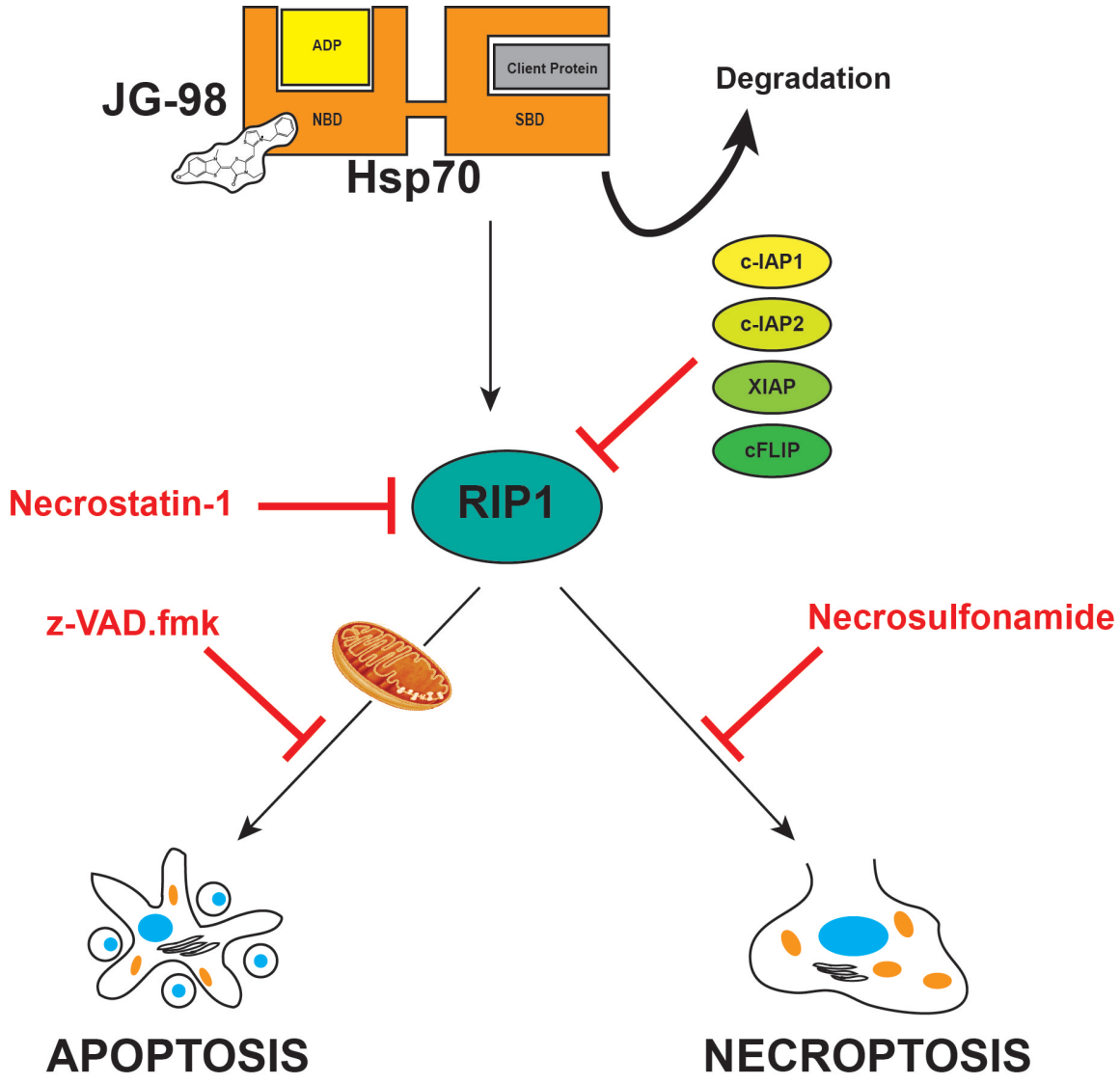

Figure 3.7 Hsp70 Guards Against Multiple Cell Death Pathways by Engaging RIP1. A model based on our data suggests that Hsp70 inhibition by JG-98 triggers RIP1's activity by directing degradation of the IAPs and cFLIP. Under most conditions, apoptosis is induced and proceeds throug the mitochondrial death pathway. However, under conditions where caspases are inactivated, RIP1 can then initiate necroptotic cell death.

3.5 Conclusion and Future Work

In conclusion, we find that JG-98, an allosteric modulator of Hsp70, reveals the chaperone's involvement in multiple cell death pathways. These results provide important insight into the roles of Hsp70 in cancer. Most strikingly, they suggest that Hsp70 functions in a much broader capacity than Hsp90. However, several questions still remain. What novel RIP1 process is being triggered by JG-98? What are the RIP1 interacting proteins that are associated after JG-98 treatment? It will be important to perform unbiased experiments to reveal how Hsp70 controls RIP1 pathways, including possible direction through the mitochondria. Does cytochrome c release depend on RIP1? Or is JG-98 capable of engaging multiple death pathways simultaneously? How does JG-98 circumvent Bcl-xL inhibition to trigger selective release of cytochrome c and not Smac? It is possible that Smac is itself a client of Hsp70 and might be degraded upon compound treatment. Experiments are currently underway to investigate all these questions.

3.6 Notes

This work, in part, has been submitted as a publication entitled “Hsp70 Regulates RIP1-Dependent Cell Death.” Sharan R. Srinivasan performed a majority of the experiments. Xiaokai Li calculated the synergistic activity of JG-98 with 17-DMAG and Bortezomib. Flow cytometry was performed by Sharan R. Srinivasan with Jooho Chung (Maillard Lab, University of Michigan). Genetically altered cell lines were prepared by Stephanie Gálban. Sharan R. Srinivasan, Xiaoki Li, Colin Duckett, and Jason Gestwicki assisted in preparation of the manuscript.

3.7 Experimental Procedures

3.7.1 Materials

Reagents:

The following reagents were purchased from Sigma-Aldrich: Necrostatin-1, Bortezomib; Enzo: z-VAD.fmk; Millipore: Necrosulfonamide; LC Labs: 17-DMAG; and Teva Pharmaceuticals: Etoposide.

Antibodies:

The following antibodies were purchased from Enzo: Hsp72 (C92F3A-5), XIAP (ADI-AAM-050), c-IAP1 (ALX-803-335), Caspase-8 (ALX-804-429); SCBT: GAPDH (sc-32233), Hsp90 (sc-7947), Raf-1 (sc-133), Caspase-8 (sc-6136), anti-rat (sc-2006), goat IgG (sc-2028); CellSignal: Akt-1 (2967), Cleaved Caspase-3 (9664), c-IAP2 (3130); BD Pharmingen: RIP1 (610459), Cdk4 (559693), cytochrome c (556433), Bcl-xL (610746); Molecular Probes: COXIV (A21347); Alexis: FLIP (ALX-804-428); Millipore: Smac (567365).

Tissue Culture

MDA-MB-231 WT cells were maintained in DMEM (Invitrogen), supplemented with 10% Fetal Bovine Serum (FBS), 1% Penicllin-Streptomycin, and non-essential amino acids. Jurkat cells were grown in RPMI 1640 (Corning), supplemented with GlutaMax. MDA-MB-231 and Jurkat cells overexpressing Bcl-xL and RIP1-KO Jurkats were all created as previously described (*51*).

3.7.2 Cell Viability Assays and Treatments

Cell death was analyzed using either the MTT Assay as previously described (*32*) or Trypan Blue Exclusion. Cells were pre-treated with z-VAD.fmk (40μM), Nec-1 (20μM), Necrosulfonamide (20μM), or a combination for 1 hour before addition of designated drug.

3.7.3 Flow Cytometry

MDA-MB-231 cells were detached using Accutase (BD Biosciences) and washed with PBS before staining with AnnexinV-APC (BD Biosciences) for 15 minutes at room temp. Cells were washed again with PBS before addition of DAPI (100μg/ml) immediately before analysis.

3.7.4 Immunoprecipitation and Western Blots

Cells were pre-treated with z-VAD.fmk (40μM) prior to compound to prevent cleavage of RIP1 upon complex activation. Following compound treatment, cells were incubate for 24 hours before proceeding with lysis, immunoprecipitation, and western blot as previously described (*32*, *41*). Cytosolic lysates were prepared using a modified digitonin extraction buffer as previously described (*52*).

3.7.5 Fluorescence Microscopy

Cells were visualized using an Olympus IX83 Inverted Microscope. Nuclear morphology was examined by Hoechst 33258 staining (Sigma).

3.8 Appendices

3.8.1 Flow Cytometry Indicates JG-98 Triggers an Apoptotic Cell Death

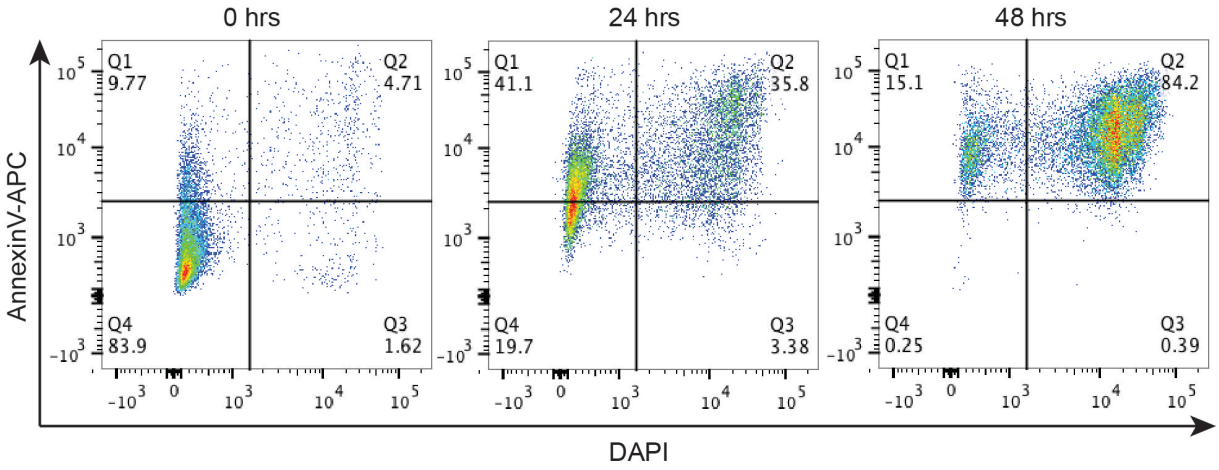

Appendix 3.1 Flow cytometry Indicates that JG-98 Triggers an Apoptotic Cell Death. MDA-MB-231 cells were treated with 10μM JG-98 for the indicated time periods. Adherent cells were trypsinized and pooled with floating cells. Samples were washed with PBS and then stained for AnnexinV-APC and DAPI before analysis on a FACS CantoII.

3.8.2 Inactivation of Both Apoptosis and Necroptosis is Required to Inactivate JG-98's Cytotoxic Effects.

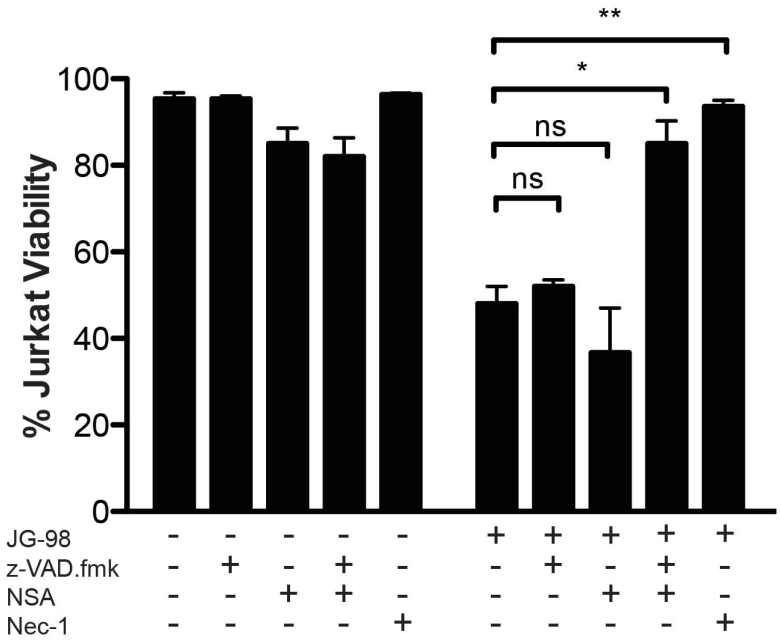

Appendix 3.2. Inactivation fo Both Apoptosis and Necroptosis is Necessary to Inhibit JG-98 Cytotoxicity. Jurkat cells were pretreated with z-VAD.fmk (40μM), Necrosulfonamide (NSA, 20μM), or Necrostatin (Nec-1, 20μM) for 1 hour prior to addition of JG-98. Inactivation of both apoptosis and necroptosis was necessary to recover cell death. Viability was determined by Trypan Blue Exclusion.

3.9 References

1. M. Ferrarini, S. Heltai, M. R. Zocchi, C. Rugarli, Unusual expression and localization of heat-shock proteins in human tumor cells, *Int J Cancer* **51**, 613–619 (1992).
2. T. M. Gress *et al.*, Differential expression of heat shock proteins in pancreatic carcinoma, *Cancer Res* **54**, 547–551 (1994).
3. J. A. Yaglom, V. L. Gabai, M. Y. Sherman, High levels of heat shock protein Hsp72 in cancer cells suppress default senescence pathways, *Cancer Res* **67**, 2373–2381 (2007).
4. M. Yano, Z. Naito, S. Tanaka, G. Asano, Expression and roles of heat shock proteins in human breast cancer, *Cancer Sci.* **87**, 908–915 (1996).
5. V. L. Gabai, K. R. Budagova, M. Y. Sherman, Increased expression of the major heat shock protein Hsp72 in human prostate carcinoma cells is dispensable for their viability but confers resistance to a variety of anticancer agents, *Oncogene* **24**, 3328–3338 (2005).
6. V. L. Gabai, J. A. Yaglom, T. Waldman, M. Y. Sherman, Heat shock protein Hsp72 controls oncogene-induced senescence pathways in cancer cells, *Mol Cell Biol* **29**, 559–569 (2009).
7. V. C. H. da Silva, C. H. I. Ramos, The network interaction of the human cytosolic 90 kDa heat shock protein Hsp90: A target for cancer therapeutics., *J. Proteomics* **75**, 2790–802 (2012).
8. J. Nylandsted, K. Brand, M. Jaattela, Heat shock protein 70 is required for the survival of cancer cells, *Ann N Y Acad Sci* **926**, 122–125 (2000).
9. C. Jolly, R. I. Morimoto, Role of the heat shock response and molecular chaperones in oncogenesis and cell death, *J Natl Cancer Inst* **92**, 1564–1572 (2000).
10. R. S. Samant, P. A. Clarke, P. Workman, The expanding proteome of the molecular chaperone HSP90, *Cell Cycle* **11**, 1301–1308 (2012).
11. M. Taipale, D. F. Jarosz, S. Lindquist, HSP90 at the hub of protein homeostasis: emerging mechanistic insights, *Nat Rev Mol Cell Biol* **11**, 515–528 (2010).
12. M. Taipale *et al.*, Quantitative analysis of HSP90-client interactions reveals principles of substrate recognition, *Cell* **150**, 987–1001 (2012).
13. J. Trepel, M. Mollapour, G. Giaccone, L. Neckers, Targeting the dynamic HSP90 complex in cancer, *Nat Rev Cancer* **10**, 537–549 (2010).
14. L. H. Pearl, C. Prodromou, P. Workman, The Hsp90 molecular chaperone: an open and shut case for treatment, *Biochem J* **410**, 439–453 (2008).
15. L. Whitesell, S. L. Lindquist, HSP90 and the chaperoning of cancer., *Nat. Rev. Cancer* **5**, 761–72 (2005).
16. J. R. Porter, C. C. Fritz, K. M. Depew, Discovery and development of Hsp90 inhibitors: a promising pathway for cancer therapy, *Curr Opin Chem Biol* **14**, 412–420 (2010).
17. N. Gaspar *et al.*, Acquired resistance to 17-allylamino-17-demethoxygeldanamycin (17-AAG, tanespimycin) in glioblastoma cells, *Cancer Res* **69**, 1966–1975 (2009).

18. S. Kummar *et al.*, Phase I trial of 17-dimethylaminoethylamino-17-demethoxygeldanamycin (17-DMAG), a heat shock protein inhibitor, administered twice weekly in patients with advanced malignancies, *Eur J Cancer* **46**, 340–347 (2010).
19. J. E. Lancet *et al.*, Phase I study of the heat shock protein 90 inhibitor alvespimycin (KOS-1022, 17-DMAG) administered intravenously twice weekly to patients with acute myeloid leukemia, *Leukemia* **24**, 699–705 (2010).
20. S. Pacey *et al.*, A phase I study of the heat shock protein 90 inhibitor alvespimycin (17-DMAG) given intravenously to patients with advanced solid tumors, *Clin Cancer Res* **17**, 1561–1570 (2011).
21. K. Jhaveri, S. Modi, HSP90 inhibitors for cancer therapy and overcoming drug resistance, *Adv Pharmacol* **65**, 471–517 (2012).
22. X. Lu, L. Xiao, L. Wang, D. M. Ruden, Hsp90 inhibitors and drug resistance in cancer: the potential benefits of combination therapies of Hsp90 inhibitors and other anti-cancer drugs, *Biochem Pharmacol* **83**, 995–1004 (2012).
23. J. Zou, Y. Guo, T. Guettouche, D. F. Smith, R. Voellmy, Repression of heat shock transcription factor HSF1 activation by HSP90 (HSP90 complex) that forms a stress-sensitive complex with HSF1, *Cell* **94**, 471–480 (1998).
24. R. Bagatell *et al.*, Induction of a Heat Shock Factor 1-dependent Stress Response Alters the Cytotoxic Activity of Hsp90-binding Agents Induction of a Heat Shock Factor 1-dependent Stress Response Alters the Cytotoxic Activity of Hsp90-binding Agents 1, *Clin Cancer Res* **6**, 3312–3318 (2000).
25. K. Nanbu *et al.*, Prognostic significance of heat shock proteins HSP70 and HSP90 in endometrial carcinomas, *Cancer Detect Prev* **22**, 549–555 (1998).
26. M. Rohde *et al.*, Members of the heat-shock protein 70 family promote cancer cell growth by distinct mechanisms., *Genes Dev.* **19**, 570–82 (2005).
27. D. R. Ciocca, S. K. Calderwood, Heat shock proteins in cancer: diagnostic, prognostic, predictive, and treatment implications, *Cell Stress Chaperones* **10**, 86–103 (2005).
28. M. V Powers, P. A. Clarke, P. Workman, Dual targeting of HSC70 and HSP72 inhibits HSP90 function and induces tumor-specific apoptosis, *Cancer Cell* **14**, 250–262 (2008).
29. E. L. Davenport *et al.*, Targeting heat shock protein 72 enhances Hsp90 inhibitor-induced apoptosis in myeloma, *Leukemia* **24**, 1804–1807 (2010).
30. D. S. Williamson *et al.*, Novel adenosine-derived inhibitors of 70 kDa heat shock protein, discovered through structure-based design, *J Med Chem* **52**, 1510–1513 (2009).
31. J. L. Brodsky, G. Chiosis, Hsp70 molecular chaperones: emerging roles in human disease and identification of small molecule modulators., *Curr. Top. Med. Chem.* **6**, 1215–25 (2006).
32. X. Li *et al.*, Analogues of the Allosteric Heat Shock Protein 70 (Hsp70) Inhibitor, MKT-077, As Anti-Cancer Agents, *ACS Med Chem Lett* **70** (2013).
33. S. Wisén, E. Bertelsen, Binding of a Small Molecule at a Protein-Protein Interface Regulates the Chaperone Activity of Hsp70-Hsp40., *ACS Chem. …* **5**, 611–622 (2010).

34. Y. Miyata *et al.*, Cysteine reactivity distinguishes redox sensing by the heat-inducible and constitutive forms of heat shock protein 70., *Chem. Biol.* **19**, 1391–9 (2012).
35. A. J. Massey *et al.*, A novel, small molecule inhibitor of Hsc70/Hsp70 potentiates Hsp90 inhibitor induced apoptosis in HCT116 colon carcinoma cells, *Cancer Chemother Pharmacol* **66**, 535–545 (2010).
36. T.-C. Chou, P. Talalay, Quantitative Analysis of Dose-Effect Relationships: The Combined Effects of Multiple Drugs or Enzyme Inhibitors, *Adv. Enzyme Regul.* **22**, 27–55 (1984).
37. S. Chandarlapaty *et al.*, SNX2112, a synthetic heat shock protein 90 inhibitor, has potent antitumor activity against HER kinase-dependent cancers., *Clin. Cancer Res.* **14**, 240–8 (2008).
38. E. Caldas-Lopes *et al.*, Hsp90 inhibitor PU-H71, a multimodal inhibitor of malignancy, induces complete responses in triple-negative breast cancer models., *Proc. Natl. Acad. Sci. U. S. A.* **106**, 8368–73 (2009).
39. D. E. Horsman, R. D. Gascoyne, R. W. Coupland, A. J. Coldman, S. A. Adomat, Comparison of cytogenetic analysis, southern analysis, and polymerase chain reaction for the detection of t(14; 18) in follicular lymphoma., *Am. J. Clin. Pathol.* **103**, 472–478 (1995).
40. D. E. Christofferson, Y. Li, J. Yuan, Control of Life-or-Death Decisions by RIP1 Kinase., *Annu. Rev. Physiol.* , 1–22 (2013).
41. T. Tenev *et al.*, The Ripoptosome, a signaling platform that assembles in response to genotoxic stress and loss of IAPs., *Mol. Cell* **43**, 432–48 (2011).
42. L. Galluzzi, O. Kepp, G. Kroemer, RIP kinases initiate programmed necrosis., *J. Mol. Cell Biol.* **1**, 8–10 (2009).
43. A. Degterev *et al.*, Identification of RIP1 kinase as a specific cellular target of necrostatins., *Nat. Chem. Biol.* **4**, 313–21 (2008).
44. A. Degterev *et al.*, Chemical inhibitor of nonapoptotic cell death with therapeutic potential for ischemic brain injury., *Nat. Chem. Biol.* **1**, 112–9 (2005).
45. M. Feoktistova *et al.*, cIAPs block Ripoptosome formation, a RIP1/caspase-8 containing intracellular cell death complex differentially regulated by cFLIP isoforms., *Mol. Cell* **43**, 449–63 (2011).
46. L. Sun *et al.*, Mixed lineage kinase domain-like protein mediates necrosis signaling downstream of RIP3 kinase., *Cell* **148**, 213–27 (2012).
47. A. R. Goloudina, O. N. Demidov, C. Garrido, Inhibition of HSP70: a challenging anti-cancer strategy., *Cancer Lett.* **325**, 117–24 (2012).
48. J. I. Leu, J. Pimkina, A. Frank, M. E. Murphy, D. L. George, A small molecule inhibitor of inducible heat shock protein 70, *Mol Cell* **36**, 15–27 (2009).
49. M. E. Murphy, The HSP70 family and cancer., *Carcinogenesis* **34**, 1181–8 (2013).
50. S. R. . Srinivasan, X. Li, J. E. Gestwicki, Allosteric Inhibitors of Hsp70: Drugging the Second Chaperone of Tumorigenesis, *Curr Top Med Chem* (2014).
51. S. Galbán *et al.*, Cytoprotective effects of IAPs revealed by a small molecule antagonist., *Biochem. J.* **417**, 765–71 (2009).
52. J. C. Wilkinson, E. Cepero, L. H. Boise, C. S. Duckett, Upstream Regulatory Role for XIAP in Receptor-Mediated Apoptosis, **24**, 7003–7014 (2004).

Chapter 4

Deconvoluting the Roles of Distinct Members of the Hsp70 Family in Cancer

4.1 Abstract

The Heat Shock Protein 70 (Hsp70) family of molecular chaperones consists of multiple members separated into subcellular compartments. It is not known whether members of the Hsp70 family play unique roles in cancer. Towards a better understanding of this question, it would be powerful to have chemical inhibitors that are selective for the various isoforms; however, this goal has been difficult to achieve. Because the binding site of MKT-077 on Hsp70s is largely conserved, we considered it unlikely that selective analogs could be designed. Rather, we took advantage of the chemical and physical properties to tune subcellular distributions of compounds. Specifically, we found that cationic molecules, such as MKT-077 or JG-98 (described in Chapters 2 and 3), are primarily targeted to the mitochondria because of their overall positive charge. Based on this finding, we describe JG-13, a neutral derivative of MKT-077, which we found to preferentially inhibit the cytosolic isoforms of Hsp70. Both JG-13 and JG-98 are cytotoxic to cancer cells and were synergistic with inhibitors of Hsp90 and the proteasome. However, treatment with JG-13 did not cause degradation of Hsp90 clients. Thus, JG-13 is a valuable addition to our chemical toolbox, and can be used to distinguish between the roles of cytoplasmic and mitochondrial Hsp70s in cancer.

4.2 Introduction

There are thirteen members of the heat shock protein 70 (Hsp70) family of proteins in humans (*1*, *2*). Members of this family are highly conserved, with sequence identity values ranging from 52-99% (*1*, *3*–*5*). Further, the biochemical properties of the Hsp70 family members, such as ATPase rate and client-binding affinity, are thought to be nearly identical. However, the members of this family are distinguished by their subcellular localization. There are specific Hsp70s found in the endoplasmic reticulum (BiP, Grp78 or HSPA5) and mitochondria (mortalin, mtHsp70, Grp75 or HSPA9). Further, the nuclear-cytoplasmic compartment also contain two major Hsp70 family members: Hsc70 (HSPA8), which is constitutively expressed and Hsp72 (HSPA1A), which is expressed in response to stress (*6*, *7*). In a few cases, specific functions have been ascribed to distinct members of this family (*8*, *9*). For example, Hsc70 appears to be important for stabilizing tau, while Hsp72 is important in tau turnover (*10*). However, it has been relatively difficult to address the question of whether Hsp70 isoforms have other unique capabilities.

As discussed in Chapter 1, Hsp70 inhibitors that compete with ATP for binding, such as Apoptozole (*11*) and VER-155008 (*12*, *13*), struggle to overcome Hsp70's high affinity for nucleotide (*14*). Furthermore, the ATP binding site is highly conserved amongst Hsp70 members and other kinases (*15*–*17*), and thus it is difficult to build selective inhibitors. One possibility is to target unique chemical functionality in the Hsp70 isoforms. For example, the Gestwicki group recently reported that methylene blue selectively inhibits Hsp72 over Hsc70, owing to the ability of this compound to oxidize a unique cysteine residue in Hsp72 (*18*). The pifithrin-μ derivative, PES, is

suggested to bind Hsp72, but not Grp75/Mortalin or Grp78/BiP (*19*, *20*). However, these results have been difficult to repeat and a recent study suggested that PES activity might be an artifact (*21*).

We reasoned that a different approach to selective inhibition of Hsp70 isoforms would be to take advantage of the intrinsic differences between the subcellular components of the cell. Specifically, it is known that MKT-077, a rhodacyanine originally shown to bind both cytosolic and mitochondrial Hsp70, is preferentially localized to the mitochondria, owing to its cationic charge and the negative potential in the organelle (*22*, *23*). Thus, although the binding site for MKT-077 on Hsp70s is highly conserved and this molecule binds multiple Hsp70s in vitro, it is likely to inhibit mtHsp70 in cells because it preferentially accumulates in that compartment. These traits are conserved in JG-98, as discussed in Chapters 2 and 3. However, we envisioned that a neutral molecule would be relatively more selective for cytosolic and (potentially) ER-resident Hsp70 members. Importantly, the charge of MKT-077 is on the pyridine ring, which was shown by NMR studies to be only peripherally involved in physical contact with Hsp70, suggesting that this region could be removed. Indeed, a previous graduate student in the Gestwicki laboratory, Yoshinari Miyata, showed that YM-08, a neutral MK-077 analog, retains affinity for Hsp70s (*24*). In this Chapter, we report the characterization of JG-13, a neutral Hsp70 inhibitor with potent anti-cancer activity. Mechanistic studies showed that JG-13 has a different mechanism-of-action than JG-98, consistent with its activity on a different subset of Hsp70 isoforms.

4.3 Results

4.3.1 Design and Development of JG-13, a Neutral Analog of MKT-077

MKT-077, though promising in pre-clinical studies, failed in Phase I Clinical Trials due to nephrotoxicity (*25*). The positive charge on the pyridinium ring was thought to contribute to renal tubular accumulation, and eventual magnesium wasting. To address this issue and create a probe for studying Hsp70s outside the mitochondria, we developed a neutral analog. Using a similar synthetic approach as employed to arrive at JG-98 (*26*), Yoshi Miyata and Xiaokai Li made modifications to MKT-077, removing the ethyl group from the pyridinium ring, yielding YM-08 (Scheme 4.1).

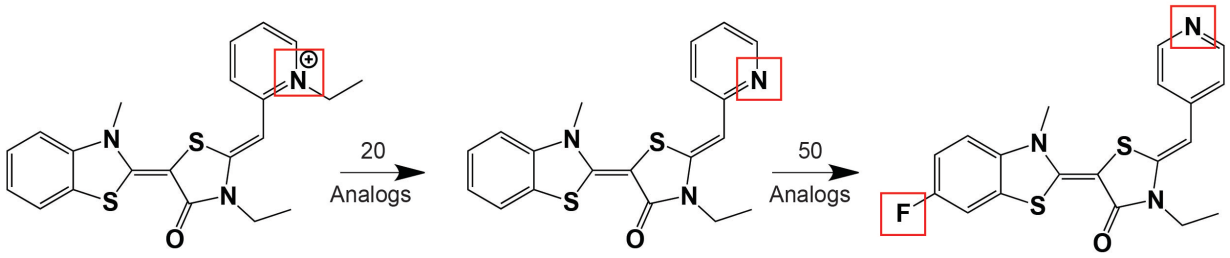

MKT-077
EC_{50} (μM) = 2.24 ± 0.18

YM-08
EC_{50} (μM) = 10.49 ± 1.86

JG-13
EC_{50} (μM) = 0.46 ± 0.08

Scheme 4.1 Development of JG-13, a potent anti-cancer compound and Hsp70 Inhibitor. Through a series of minor structural changes to the rhodocyanine MKT-077, we synthesized neutral analogs. YM-08 retained binding to the chaperone (data not shown), but lacked potency. Several more modfiications led to JG-13, a neutral analog with potent chaperone inhibition and anti-cancer activity. IC50 values shown are against MCF-7 cells.

Though not particularly effective as an anti-cancer agent, YM-08 retained its ability to bind Hsp70 and, more importantly, was not retained in mouse kidneys (*24*). It also showed penetrance into the brain, suggesting potential uses for a neutral MKT-077 derivative in neurological malignancies.

Starting from YM-08, and using insights learned from studies with charged analogs (see Chapter 2), we made several more analogs to improve pharmacokinetic and -dynamic features. Fluorination of the benzothiazole ring greatly improved compound stability, similar to JG-98, by blocking CYP450 oxidation sites. We next rotated the heteroatom of the pyridine ring from the 2- to 4- position, which greatly improved potency. In fact, JG-13 yielded EC_{50} values against MCF-7, MDA-MB-231, and HeLa cells that are similar, if not better, to those of JG-98 (~300-400 nM; Figures 4.1.A-C). Compared to JG-98, JG-13 was more toxic to MEFs (Figure 4.1.D), although the therapeutic index was still favorable (>20).

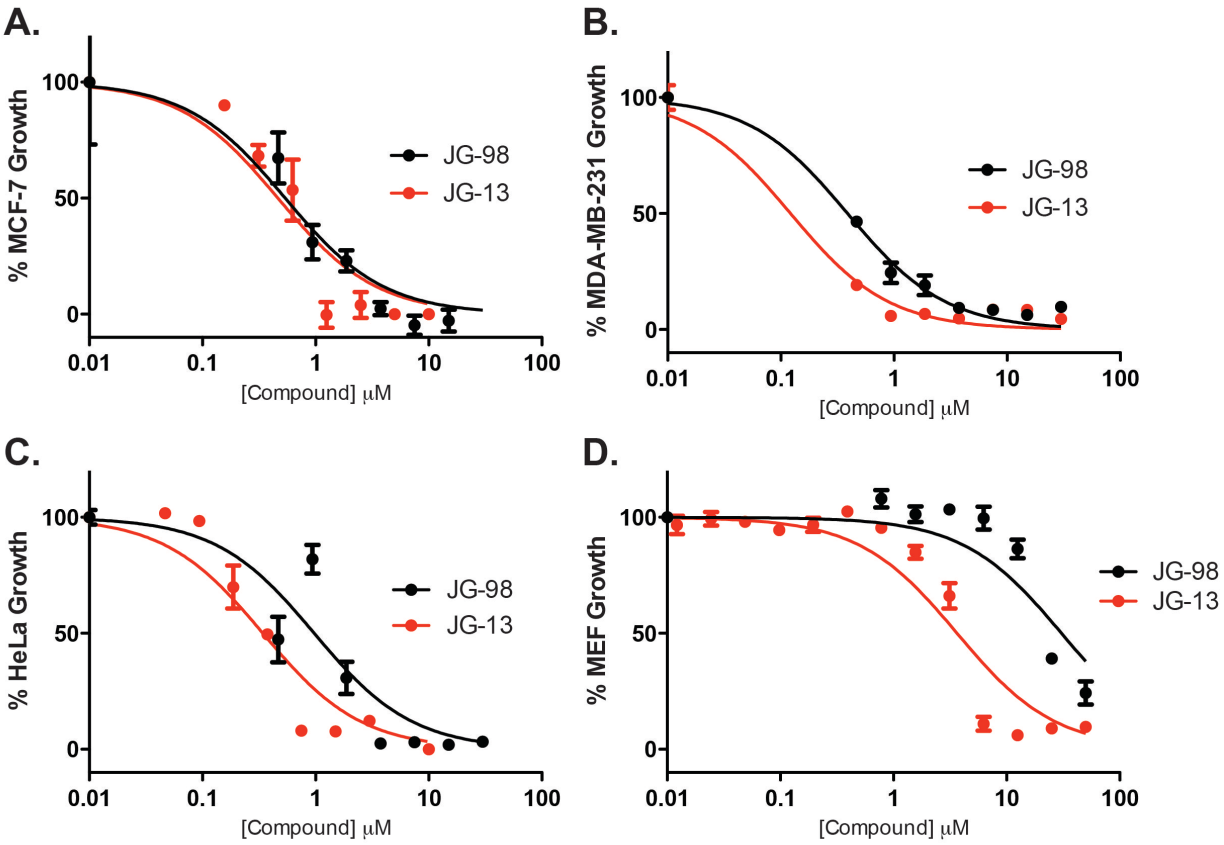

Figure 4.1 JG-13 Displays Increased Toxicity over JG-98. JG-13 displays improved EC50 values against MCF-7 **(A)**, MDA-MB-231 **(B)**, and HeLa **(C)** cell lines. **(D)** JG-13 is more toxic to MEFs compared to JG-98, but still exhibits a favorable therapeutic index (>20).

4.3.2 Genomic shRNA Screen Reveals JG-13 Targets Cytoplasmic Hsp70

We next sought to determine how much of the anti-proliferative activity of JG-13 might arise from inhibition of cytosolic members of the Hsp70 family. Collaborating with Jonathan Weissman (UCSF), we performed a genomic shRNA screen (*27*) against 1,000 PQC targets, scanning for sensitization or resistance to sublethal doses of JG-13. Knockdown of cytosolic Hsp70, but not mitochondrial Hsp70, sensitized the cells to JG-13 treatment (Weissman Lab, UCSF). Conversely, cationic molecules, such as JG-84 and JG-98, were more sensitive to knockdown of mtHsp70 (as discussed in Chapter 2). Together, these results support the idea that neutral analogs are relatively selective for cytoplasmic Hsp70s, while cationic ones are more dependent on mtHsp70. Work to confirm this selectivity in biochemical assays is currently underway. Importantly, a small number of other genes appeared to sensitize cells to treatment with JG-13, including DjC13, a member of the Hsp40 family. Further work will have to be done to confirm the relative importance of these factors. Despite this ongoing work, we decided to pursue the use of JG-13 and JG-98 and characterize the similarities and differences between the cellular responses to these chemical probes.

4.3.3 JG-13 Traps Hsp70 in an ADP-Bound State, Similar to Other MKT-077 Derivatives.

To confirm whether JG-13 might bind Hsp70 in the same conserved, allosteric pocket as MKT-077, we used molecular modeling and docking simulations to predict whether this compound would interact in this region. Similar to what we observed with MKT-077 and JG-98 (see Chapter 2), we found that JG-13 binds to the same allosteric pocket with a similar orientation to the cationic molecules (Figure 4.2.A).

Based on the docked model, we would expect that JG-13 would inhibit the activity of Hsp70s *in vitro*. To test this idea, we tested JG-13 for activity in these assays and confirmed that it suppressed J-protein stimulated ATPase activity of Hsp70 (Figure 4.2.B). Moreover, we found that JG-13 disrupted binding between Hsp70 and a nucleotide exchange factor (NEF) co-chaperone, BAG3 (Figure 4.2.C). Thus, JG-13 appeared to retain many of the features of the cationic Hsp70 inhibitors, with a similar potency to JG-98.

A. JG-13 Binds an Allosteric Pocket on Hsp70 NBD

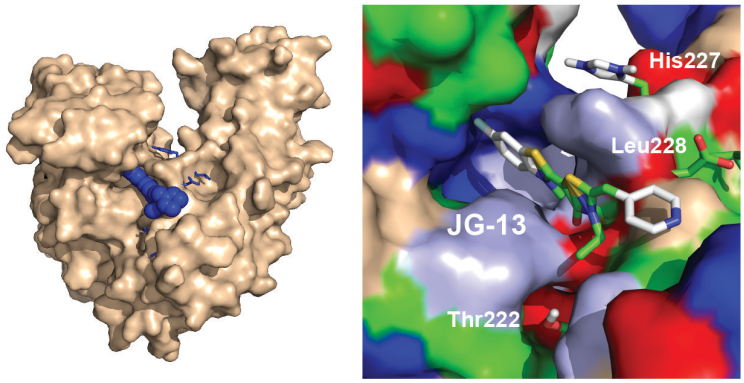

B. JG-13 Inhibits J-protein Stimulated ATPase Activity

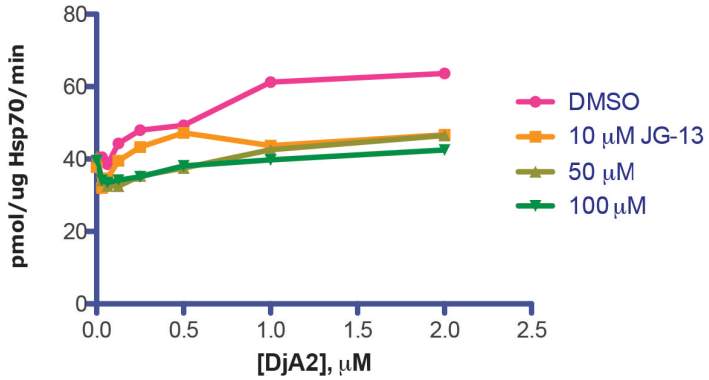

C. JG-13 Disrupts Interaction Between Hsp70 and Bag3

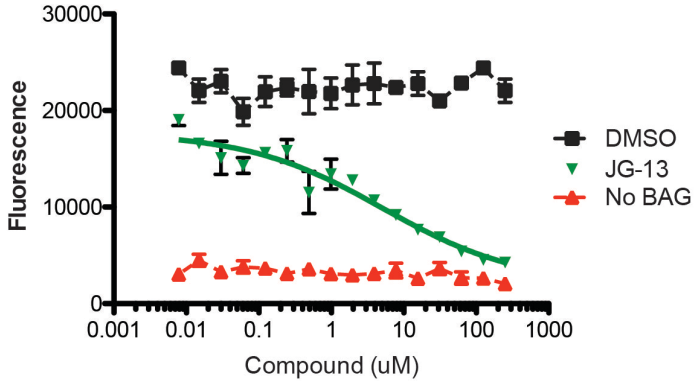

Figure 4.2 JG-13 Traps Hsp70 in the ADP-Bound State
(A). Left: JG-13 (blue spheres) binds to a pocket opposite the ATP-binding site of Hsp70. Right: Close-up of binding pose. Hsp70 residues are colored as follows: (green: A,C,F,I,L,M,P; light blue: T,Y; blue: H,K,R; red: D,E; wheat: G,N,Q,S).**(B)** JG-13 inhibits ability of J-protein (DjA2) to stimulate ATPase rate of Hsp70. **(C)** Biotin-Hsp70 was immobilized onto streptavidin coated beads. Alexa488-labeled Bag3 was then incubated with Hsp70 in the presence of JG-13 at varying concentrations. % Binding was determined by fluorescence.

4.3.4 JG-13 Induces Apoptotic Features

Similar to JG-98, we found that JG-13 induced apoptosis in MDA-MB-231 cells, based on annexinV and DAPI staining (Figure 4.3.A). Specifically, the treated cells progressed from double negative to annexinV+/DAPI- to double positive over 24 hours Cell death in response to JG-13 was relatively rapid, closely paralleling the kinetics of JG-98 (Appendix 4.1).

Interestingly, we noticed that cells treated with JG-13 had different morphological features than those treated with JG-98. For example, MDA-MB-231 cells treated with JG-13 lacked hallmark features of apoptosis, such as membrane blebbing and cell shrinkage (Figure 4.3.B). We also saw discrete, fluorescent punctae, which might occur from intracellular accumulation of JG-13. Future work is needed to determine whether these puncta co-localize with autophagosomes, lysosomes or some other structure. However, these studies were the first evidence that JG-13 and JG-98 might be killing cancer cells by different mechanisms.

A. JG-13 Induces an Apoptotic-Like Profile by Flow Cytometry

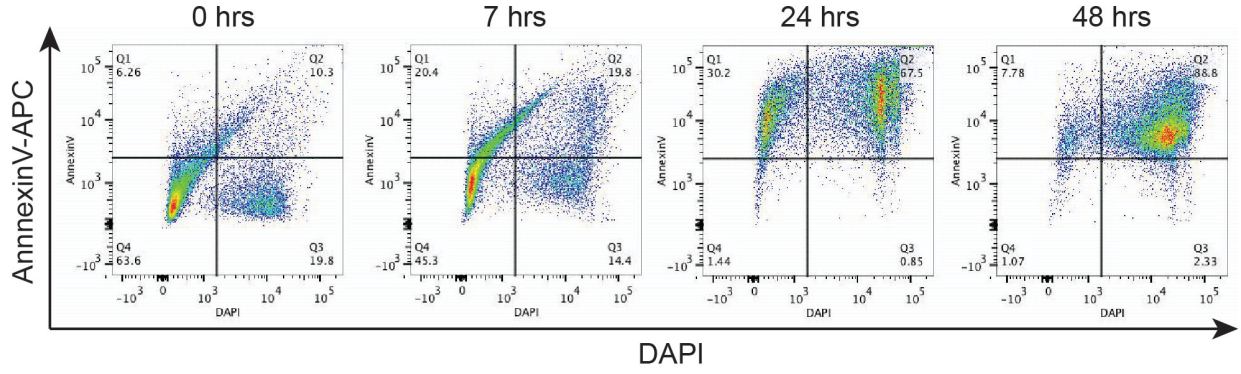

B. Microscopy Reveals a Unique Morphological Phenotype

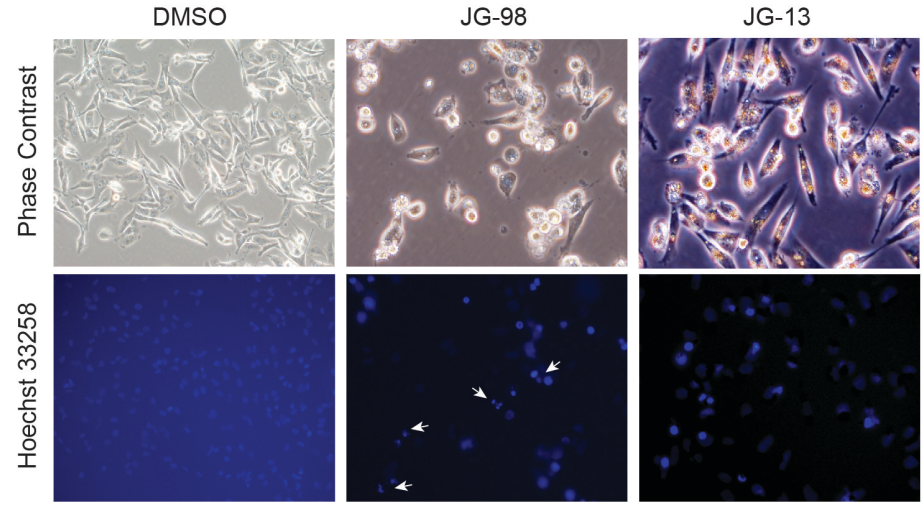

Figure 4.3 JG-13 Induces a Cell Death with a Unique Profile. (A) MDA-MB-231 cells were treated with 10μM JG-13 for indicated time periods before being detached, washed, and analyzed by flow cytometry for AnnexinV and DAPI staining. Progression of AV-/DAPI- to AV+/DAPI- to AV+/DAPI+ is consistent with an apoptotic profile. (B) MDA-MB-231 cells were treated for 24 hours with DMSO, 10μM JG-98, or 10μM JG-13. Nuclear morphology was examined by Hoechst stain for 30 min prior to microscopy.

4.3.5 Hsp90 Clients are Relatively Unaffected by JG-13 Treatment

To further understand the differences between the charged and neutral compounds, we turned to examine the molecular changes exerted by JG-13. As mentioned in Chapter 3, MKT-077 is known to relieve inhibition of p53 (*28*). Similarly, we found that JG-83 stabilized wild type p53 in MCF-7 cells. However, treatment with JG-13 seemed to trigger degradation of the tumor suppressor (Figure 4.4.A). Additionally, while JG-98 led to loss of Hsp90 clients, such as Akt, Raf-1, and Cdk4, JG-13 was relatively inactive (although some degradation of Raf-1 was seen) (Figure 4.4.B). Further, JG-13 did not activate caspase-3 or PARP cleavage (Appendix 4.2). Thus, although JG-13 triggers a cell death with some apoptotic features, its exact mechanism of action is considerably different than that of JG-98. These results suggest that Hsp70s are not all redundant in maintaining cancer cells. Rather, mtHsp70 and the cytoplasmic isoforms appear to play distinct roles.

A. JG-13 Cytotoxicity is Independent of p53 in MCF-7 Cells

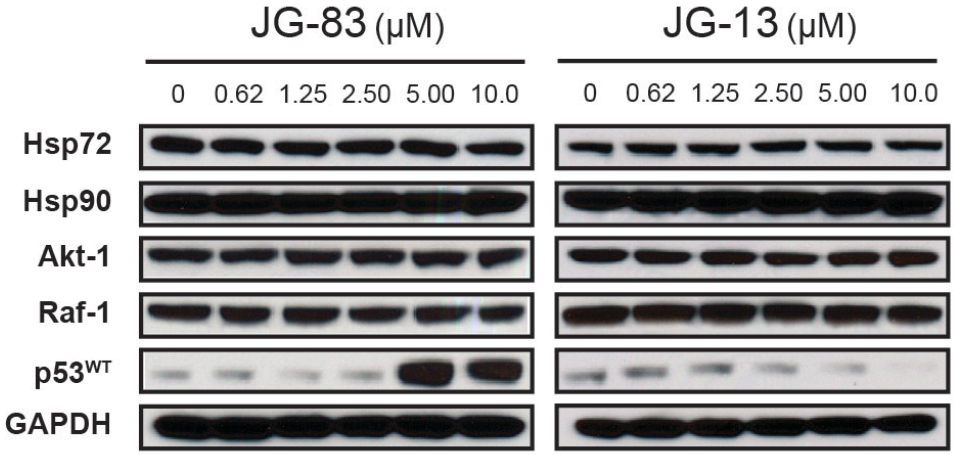

B. JG-13 Modestly Affects Hsp90 Clients in MDA-MB-231 Cells

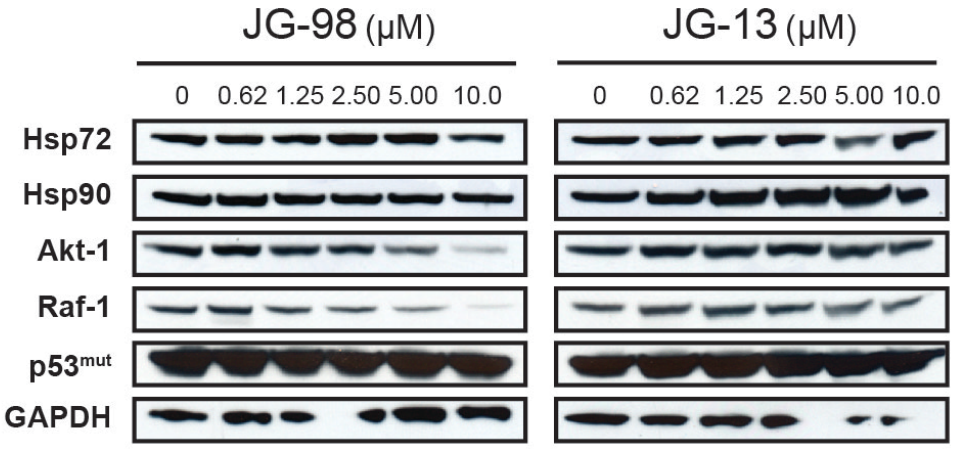

Figure 4.4 JG-13 Differs from Charged MKT-077 Derivatives in effects on Hsp90 Clients. (A) Contrary to charged analogs, JG-13 induces degradation of p53 in MCF-7 cells. **(B)** JG-13 has a modest effect on Hsp90 clients in MDA-MB-231 cells, though not as pronounced as charged analogs.

4.3.6 JG-13 is Synergistic with Other Drugs Targeting PQC Machinery

Given JG-98's synergistic activity with both Hsp90 and proteasome inhibitors, we sought to determine if JG-13 might have similar qualities. Using the MTT assay, we found that JG-13 was highly synergistic with 17-DMAG in MCF-7 cells (Figure 4.5.A). However, JG-13 did not appear to be synergistic with Bortezomib (Figure 4.5.B). In fact, JG-13 seemed to weaken the activity of Bortezomib in some cases. These results were another indication that the mechanism of cell death through the Hsc70/Hsp72 system was distinct. To test this idea in more detail, we asked whether JG-13 would be synergistic with JG-83, a charged derivative similar to JG-98. We found that the two analogs of MKT-077 had potent synergy (Figure 4.5.C), supporting the model that they target different Hsp70s. Moreover, these results suggest that combination therapy, employing inhibitors of multiple Hsp70s, might be a viable avenue for future therapeutic intervention.

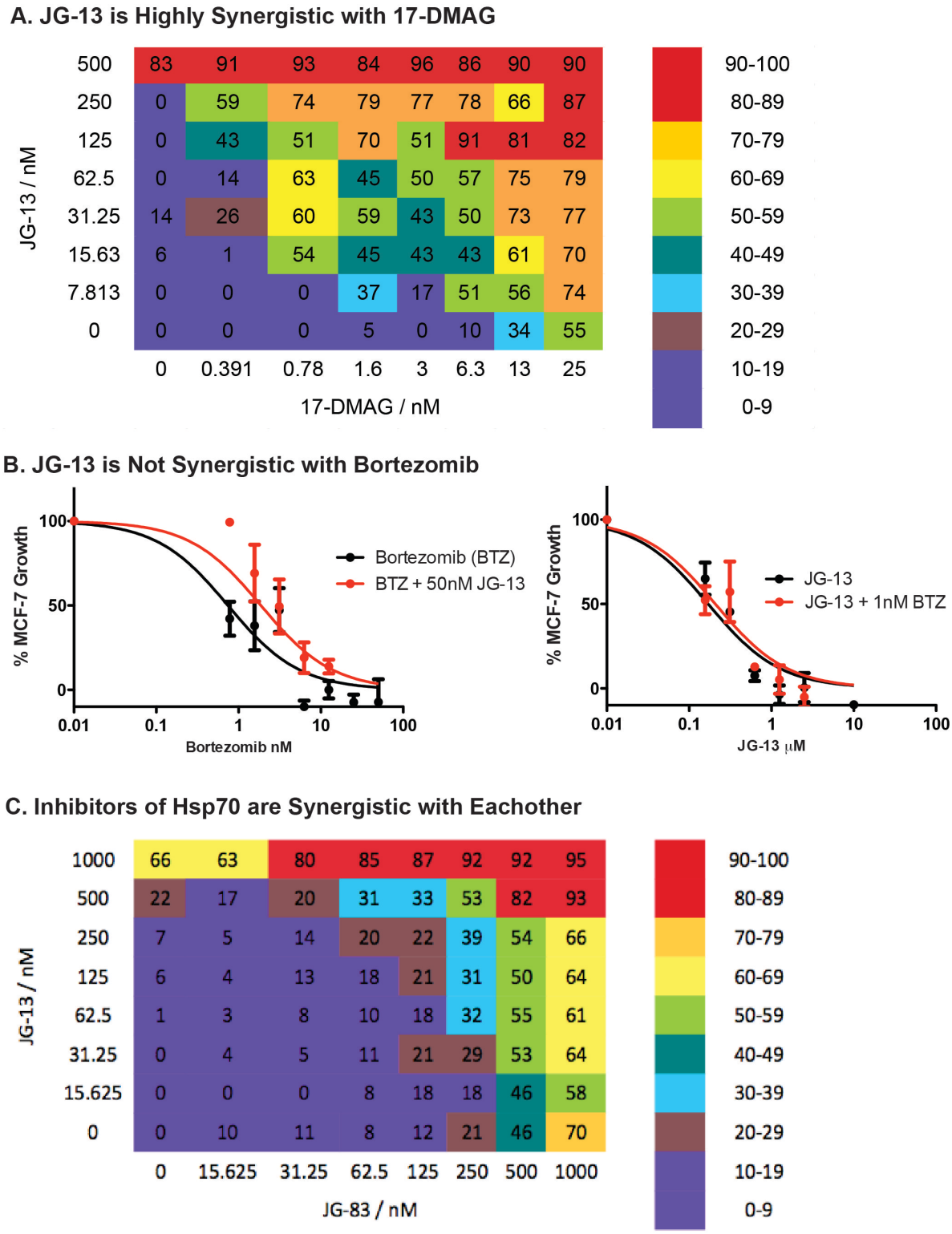

Figure 4.5 Synergistic Activity of JG-13 with Other Inhibitors of PQC Machinery. (A) Heat map detailing synergism between JG-13 and 17-DMAG. **(B)** JG-13 does not exhibit increased activity in the presence of Bortezomib. **(C)** Heat map detailing synergism bewteen JG-13 and JG-83, a charged analog of MKT-077. Viability was determined using the MTT assay. All measurements were obtained in MCF-7 cells.

4.4 Discussion

Cationic molecules, such as MKT-077 and JG-98 preferentially distribute to the mitochondria, where the electron potential is strongly negative (*23*). Consistent with this idea, the cytotoxicities of MKT-077, JG-84 and JG-98 were sensitive to the levels of mortalin/mtHsp70. However, biochemical pulldown experiments with immobilized MKT-077 have shown that this compound also interacts with cytoplasmic Hsc70 (*28*). These results suggest that JG-98 and its cationic analogs are likely to interact with multiple Hsp70 isoforms, but that mortalin/mtHsp70 might play an important role in its cytotoxicity mechanism. Clearly, more work is needed to quantify the selectivity of JG-98. As a step towards deconvoluting the effects of JG-98, we developed a neutral analog of MKT-077, JG-13. We reasoned that this molecule might be used to differentiate between the effects of MKT-077 analogs mediated by the cationic charge properties from the possibility of pan-Hsp70 activity.

Initial efforts to convert MKT-077 into a neutral molecule focused on removing the ethyl functionalization of the pyridine ring, yielding YM-08. Though this molecule had weak anti-cancer activity, YM-08 served as a useful intermediate to justify efforts at producing neutral MKT-077 analogs. For example, YM-08 retained affinity for Hsp70 and it suppressed Hsp70's ATPase activity *in vitro*. Further, it did not show any significant accumulation in the kidneys (this was important because the clinical evaluation of MKT-077 was abandoned due to renal toxicity in a subset of patients) and it crossed the blood brain barrier, suggesting a potential future use for these compounds in neurological malignancies.

By adding a fluorine group to the metabolically labile benzothiazole ring, and rotating the pyridine ring to the para position, we obtained JG-13, a neutral YM-08 analog with increased stability in P_{450} assays and improved anti-cancer activity. Importantly, JG-13, like other MKT-077 analogs, trapped Hsp70 in an ADP-bound state, with a low affinity for NEF co-chaperones. Further, docking studies supported the idea that JG-13 binds the same pocket as MKT-077, JG-98 and other analogs. This finding is expected because the cationic pyridine does not appear to make direct favorable contacts with Hsp70. Rather, the benzothiazole ring of these molecules is inserted into a deep, hydrophobic pocket in the enzyme. Thus, removing the charged pyridinium does not weaken affinity for the target.

A genomic shRNA screen revealed that knockdown of cytoplasmic Hsp70 sensitized cells to JG-13, as compared to mortalin/mtHsp70 for JG-98 (see Chapter 2). Thus, JG-13 appears to target the cytoplasmic pool of Hsp70, though it is difficult to rule out activity against other Hsp70s in the absence of supportive biochemical data. Another graduate student in the Gestwicki laboratory will be exploring the selectivity of these molecules in greater detail. Despite these questions, we sought to characterize the cellular responses to JG-13 and JG-98 to gain an initial understanding of the potential differences between Hsc70/Hsp72 and mtHsp70 in cancer.

There were some similarities in the response of cells to JG-13 and JG-98. For example, neither compound activated a stress response and both had potent anti-proliferative activity (EC_{50} ~200 to 400 nM). However, while JG-83 caused a dramatic stabilization of p53 in MCF-7 ($p53^{+/+}$) cells, JG-13 actually seemed to induce

degradation of the tumor suppressor. Further, there was little change in the levels of Akt, Cdk4, or Raf-1 in either MCF-7 or MDA-MB-231 cells upon JG-13 treatment.

To further understand the cytotoxicity of JG-13, we turned to flow cytometry and found that the treated cells had an apoptotic profile by annexin staining. However, there was a lack of apoptotic features by microscopy. Instead, discrete, fluorescent punctae were formed in response to JG-13. Future work will clarify the identity of these additional features (see Chapter 5). Preliminary data showed a modest conversion of LC3-I to active LC3-II in MCF-7 cells (Appendix 4.2), suggesting that autophagy could be one viable mechanism. Cytoplasmic Hsp70s are well known to stabilize lysosomes (*29*), further suggesting this possibility. Pre-treatment of cells with necrostatin-1, an inhibitor of RIP1's kinase activity, partially recovered viability in JG-13 treated cells (Appendix 4.3). Thus, as a preliminary model, we suggest that JG-13 might triggers a RIP1-dependent, autophagic pathway. Exactly how these pathways connect will be the subject of future studies.

Lastly, we examined the synergistic nature of JG-13 with other compounds targeting the protein quality control machinery. As with JG-98, JG-13 was highly active in combination with 17-DMAG. Interestingly, JG-13 was not synergistic with bortezomib, further suggesting a unique mechanism compared to the charged analogs. Further, JG-13 was synergistic with JG-83 and other charged derivatives. Together, these results suggest that JG-13 and JG-98 target distinct pools of Hsp70s. These results also suggest that targeting multiple Hsp70 isoforms may be a favorable therapeutic strategy.

4.5 Conclusion

There are thirteen Hsp70s in most cells, yet little is known about how these isoforms might play distinct roles. Further, little is known about which isoform(s) might be the best anti-cancer targets. Rather than develop molecules that are able to distinguish between structural features amongst the highly conserved Hsp70 isoforms, we chose to modify a single scaffold, MKT-077. We tuned the electronic properties of this scaffold to generate an analog, JG-13, that is not localized to mitochondria. For the first time, we are able to show a pharmacological difference between the dependence of cancer cells on these pools of Hsp70s. Specifically, JG-98 and JG-13 initiate cell death by very different pathways, suggesting that the multiple Hsp70 isoforms cooperate to guard against diverse routes to cell death. Future work combining JG-98 and JG-13 along with genetic knockdowns will help identify the exact roles played by the specific Hsp70 family members.

4.6 Notes

Sharan R. Srinivasan performed a majority of the experiments, including viability, docking, synergy, and cytotoxic mechanism studies. Synthesis of neutral derivatives of MKT-077 was performed by Yoshinari Miyata and Xiaokai Li. Jooho Chung assisted with flow cytometry of MDA-MB-231 cells. Jennifer N. Rauch and Zapporah T. Young examined disruption of Hsp70-Bag3 Binding. Sharan R. Srinivasan and Jason E. Gestwicki contributed to the preparation of this manuscript.

4.7 Experimental Procedures

4.7.1 Materials

Reagents:

The following reagents were purchased from Sigma-Aldrich: Necrostatin-1, Bortezomib; Enzo: z-VAD.fmk; Millipore: Necrosulfonamide; LC Labs: 17-DMAG.

Antibodies:

The following antibodies were purchased from Enzo: Hsp72 (C92F3A-5); SCBT: GAPDH (sc-32233), Hsp90 (sc-7947), Raf-1 (sc-133), p53 (DO-1), p62 (sc-28359), Actin (sc-47778); CellSignal: Akt-1 (2967), Caspase-3 (9662), Cdk4 (2906), PARP (9542); Novus: LC3 (NB100-2331).

4.7.2 Tissue Culture

MDA-MB-231 WT cells were maintained in DMEM (Invitrogen), supplemented with 10% Fetal Bovine Serum (FBS), 1% Penicllin-Streptomycin, and non-essential amino acids. Jurkat cells were grown in RPMI 1640 (Corning), supplemented with GlutaMax. MDA-MB-231 and Jurkat cells overexpressing Bcl-xL and RIP1-KO Jurkats were all created as previously described (*30*).

4.7.3 Cell Viability Assays and Treatments

Cell death was analyzed using either the MTT Assay as previously described (*26*) or Trypan Blue Exclusion. Cells were pre-treated with z-VAD.fmk (40μM), Nec-1 (20μM), Necrosulfonamide (20μM), or a combination for 1 hour before addition of designated drug.

4.7.4 Flow Cytometry

Cell-Based: MDA-MB-231 cells were detached using Accutase (BD Biosciences) and washed with PBS before staining with AnnexinV-APC (BD Biosciences) for 15 minutes at room temp. Cells were washed again with PBS before addition of DAPI (100μg/ml) immediately before analysis.

Protein-Interaction: Biotinylated Hsp72 was immobilized on polysterene streptavidin coated beads (Spherotech), incubated with Alexa-Fluor® 488 labeled BAG3 (50nM) and increasing amounts of JG-13 in buffer A (25mM HEPES, 5mM $MgCl_2$, 10mM KCl, 0.3% Tween-20 pH 7.5). Plates were incubated for 15 minutes then analyzed using a Hypercyt liquid sampling unit in line with an Accuri® C6 Flow Cytometer. Protein complex inhibition was detected by measuring median bead associated fluorescence. DMSO was used as a negative control and 1μM excess unlabeled Hsp70 was used as a positive control.

4.7.4 Fluorescence Microscopy

Cells were visualized using an Olympus IX83 Inverted Microscope. Nuclear morphology was examined by Hoechst 33258 staining (Sigma).

4.7.5 Molecular Modeling and Docking

Computational modeling of JG-13 binding to $Hsc70_{NBD}$ (PDB: 3C7N) was obtained using similar methods as previously described (*24*, *31*). Briefly, AUTODOCK-4.2 was used for the docking of JG-13 to $Hsc70_{NBD}$ with the following parameters: GA runs = 100, initial population size = 1500, max number of evaluations = long, max number of surviving top individuals = 1, gene mutation rate = 0.02, rate of crossover = 0.8, GA crossover mode: two points, Cauchy distribution mean for gene mutation = 0, Cauchy distribution variance for gene mutation = 1, number of generations for picking worst individuals = 10. The docked structures were clustered and then evaluated using PyMol. All calculations were completed on a Apple MacBookPro computer equipped with a 64-bit 2.4 GHz Intel Core 2 Duo processor running MacOSX 10.6.8.

4.8 Appendices

4.8.1 JG-13 Induces a Rapid Cell Death

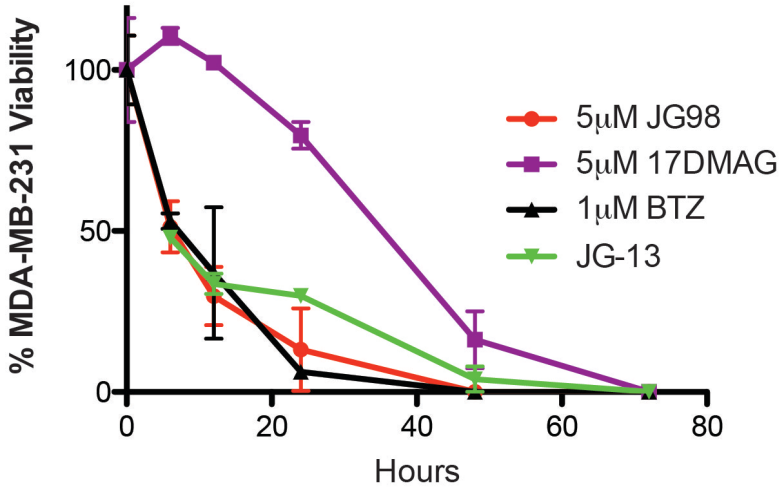

Appendix 4.1 JG-13 Elicits a Rapid Cell Death. Treatment with of MDA-MB-231 cells with JG-13 results in a rapid cell death, similar to JG-98.

4.8.2 JG-13 Mildly Affects Hsp90 Clients

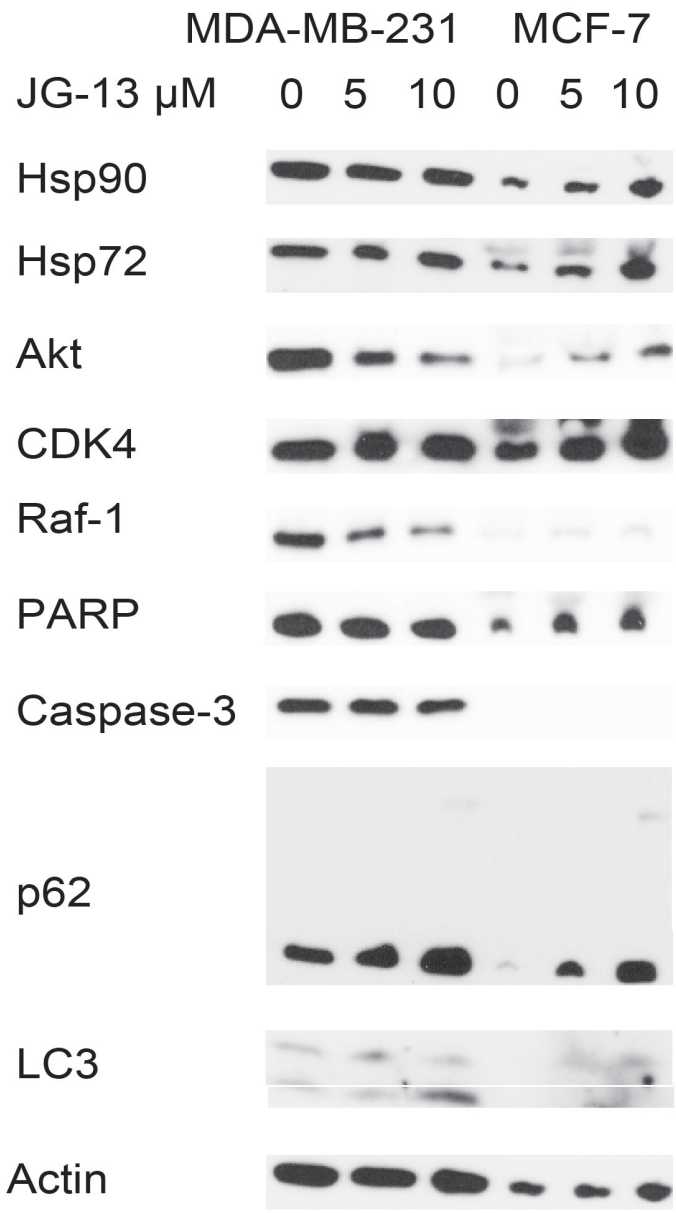

Appendix 4.2 JG-13 Mildly Affects Hsp90 Clients. Treatment with JG-13 results in modest degradation of Hsp90 clients, Akt, and Raf-1. Caspase-3 and PARP cleavage are absent. MDA-MB-231 cells show some conversion of LC3, suggesting possible involvement in autophagy.

4.8.3 JG-13 is At Least Partially Dependent on RIP1 Kinase Activity

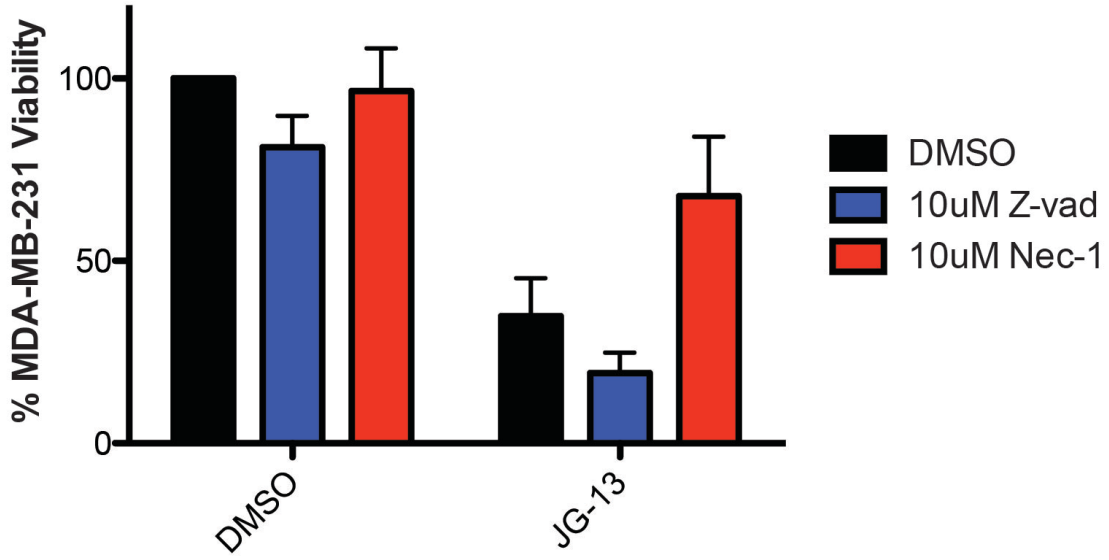

Appendix 4.3 Necrostatin-1 Partially Recovers JG-13 Cytotoxicity. Pre-treatment of MDA-MB-231 cells with z-VAD.fmk did not recover cell death, while inhibiting RIP1 Kinase activity with Necrostatin-1 partially restored viability.

4.9 References

1. J. Hageman, M. a W. H. van Waarde, A. Zylicz, D. Walerych, H. H. Kampinga, The diverse members of the mammalian HSP70 machine show distinct chaperone-like activities., *Biochem. J.* **435**, 127–42 (2011).
2. M. Rohde *et al.*, Members of the heat-shock protein 70 family promote cancer cell growth by distinct mechanisms., *Genes Dev.* **19**, 570–82 (2005).
3. W. Boorstein, T. Ziegelhoffer, E. Craig, Molecular evolution of the HSP70 multigene family, *J. Mol. Evol.* **38** (1994), doi:10.1007/BF00175490.
4. R. Gupta, G. B. Golding, Evolution of HSP70 gene and its implications regarding relationships between archaebacteria, eubacteria, and eukaryotes, *J. Mol. Evol.* **37** (1993), doi:10.1007/BF00182743.
5. S. Karlin, L. Brocchieri, Heat Shock Protein 70 Family: Multiple Sequence Comparisons, Function, and Evolution, *J. Mol. Evol.* **47**, 565–577 (1998).
6. C. V Dang, W. M. Lee, Nuclear and nucleolar targeting sequences of c-erb-A, c-myb, N-myc, p53, HSP70, and HIV tat proteins., *J. Biol. Chem.* **264**, 18019–18023 (1989).
7. D. Ciocca *et al.*, Heat shock proteins hsp27 and hsp70: lack of correlation with response to tamoxifen and clinical course of disease in estrogen receptor-positive metastatic breast cancer (a Southwest Oncology Group Study), *Clin. Cancer Res.* **4**, 1263–1266 (1998).
8. J. Hageman, H. H. Kampinga, Computational analysis of the human HSPH/HSPA/DNAJ family and cloning of a human HSPH/HSPA/DNAJ expression library., *Cell Stress Chaperones* **14**, 1–21 (2009).
9. M. Daugaard, M. Rohde, M. Jäättelä, The heat shock protein 70 family: Highly homologous proteins with overlapping and distinct functions*FEBS Lett.* **581**, 3702–3710 (2007).
10. U. K. Jinwal *et al.*, Imbalance of Hsp70 family variants fosters tau accumulation., *FASEB J.* **27**, 1450–9 (2013).
11. D. R. Williams, S. K. Ko, S. Park, M. R. Lee, I. Shin, An apoptosis-inducing small molecule that binds to heat shock protein 70, *Angew Chem Int Ed Engl* **47**, 7466–7469 (2008).
12. D. S. Williamson *et al.*, Novel adenosine-derived inhibitors of 70 kDa heat shock protein, discovered through structure-based design, *J Med Chem* **52**, 1510–1513 (2009).
13. A. J. Massey *et al.*, A novel, small molecule inhibitor of Hsc70/Hsp70 potentiates Hsp90 inhibitor induced apoptosis in HCT116 colon carcinoma cells, *Cancer Chemother Pharmacol* **66**, 535–545 (2010).
14. A. J. Massey, ATPases as drug targets: insights from heat shock proteins 70 and 90, *J Med Chem* **53**, 7280–7286 (2010).
15. K. M. Flaherty, C. DeLuca-Flaherty, D. B. McKay, Three-dimensional structure of the ATPase fragment of a 70K heat-shock cognate protein., *Nature* **346**, 623–628 (1990).

16. L. Brocchieri, E. Conway de Macario, A. J. L. Macario, hsp70 genes in the human genome: Conservation and differentiation patterns predict a wide array of overlapping and specialized functions., *BMC Evol. Biol.* **8**, 19 (2008).
17. A. Buchberger, H. Schröder, M. Büttner, A. Valencia, B. Bukau, A conserved loop in the ATPase domain of the DnaK chaperone is essential for stable binding of GrpE, *Nat. Struct. Biol.* **1**, 95–101 (1994).
18. Y. Miyata *et al.*, Cysteine reactivity distinguishes redox sensing by the heat-inducible and constitutive forms of heat shock protein 70., *Chem. Biol.* **19**, 1391–9 (2012).
19. J. I. Leu, J. Pimkina, A. Frank, M. E. Murphy, D. L. George, A small molecule inhibitor of inducible heat shock protein 70, *Mol Cell* **36**, 15–27 (2009).
20. J. I. Leu, J. Pimkina, P. Pandey, M. E. Murphy, D. L. George, HSP70 inhibition by the small-molecule 2-phenylethynesulfonamide impairs protein clearance pathways in tumor cells, *Mol Cancer Res* **9**, 936–947 (2011).
21. R. Schlecht *et al.*, Functional Analysis of Hsp70 Inhibitors., *PLoS One* **8**, e78443 (2013).
22. B. G. Heerdt, M. A. Houston, L. H. Augenlicht, The intrinsic mitochondrial membrane potential of colonic carcinoma cells is linked to the probability of tumor progression., *Cancer Res.* **65**, 9861–7 (2005).
23. M. R. Duchen, Contributions of mitochondria to animal physiology: from homeostatic sensor to calcium signalling and cell death, *J. Physiol.* **516**, 1–17 (1999).
24. Y. Miyata *et al.*, Synthesis and Initial Evaluation of YM-08, a Blood-Brain Barrier Permeable Derivative of the Heat Shock Protein 70 (Hsp70) Inhibitor MKT-077, Which Reduces Tau Levels., *ACS Chem. Neurosci.* , 8–10 (2013).
25. C. Britten, E. Rowinsky, S. Baker, A phase I and pharmacokinetic study of the mitochondrial-specific rhodacyanine dye analog MKT 077, *Clin. cancer …* , 42–49 (2000).
26. X. Li *et al.*, Analogues of the Allosteric Heat Shock Protein 70 (Hsp70) Inhibitor, MKT-077, As Anti-Cancer Agents, *ACS Med Chem Lett* **70** (2013).
27. M. Kampmann, M. C. Bassik, J. S. Weissman, Integrated platform for genome-wide screening and construction of high-density genetic interaction maps in mammalian cells., *Proc. Natl. Acad. Sci. U. S. A.* **110**, E2317–26 (2013).
28. R. Wadhwa, T. Sugihara, A. Yoshida, H. Maruta, S. C. Kaul, Selective Toxicity of MKT-077 to Cancer Cells Is Mediated by Its Binding to the hsp70 Family Protein mot-2 and Reactivation of p53 Function Advances in Brief Selective Toxicity of MKT-077 to Cancer Cells Is Mediated by Its Binding to the hsp70 Family Prot, , 6818–6821 (2000).
29. T. Kirkegaard *et al.*, Hsp70 stabilizes lysosomes and reverts Niemann-Pick disease-associated lysosomal pathology., *Nature* **463**, 549–53 (2010).
30. S. Galbán *et al.*, Cytoprotective effects of IAPs revealed by a small molecule antagonist., *Biochem. J.* **417**, 765–71 (2009).
31. A. Rousaki *et al.*, Allosteric drugs: the interaction of antitumor compound MKT-077 with human Hsp70 chaperones, *J Mol Biol* **411**, 614–632 (2011).

Chapter 5

Conclusions and Future Directions: Unraveling the Signaling Roles of Hsp70 in Cancer and Development of Hsp70 Inhibitors as Therapeutics

5.1 Abstract

In the preceding chapters, the development of small molecules targeting Hsp70 was described and these molecules were shown to be potent anti-cancer agents. In addition, these studies have advanced our understanding of the roles Hsp70 plays in maintaining the cancer phenotype. Most significantly, we showed that Hsp70 has a previously unanticipated activity as a hub of multiple cell death pathways. Additionally, we have started to define how individual Hsp70 family members might play discrete roles in cell survival. However, many questions still remain. What RIP1-dependent process is being controlled by Hsp70? How do the individual Hsp70 isoforms contribute to the various cell death pathways? This chapter proposes some of the future studies that will shed light on these questions. In addition, we discuss the implications of this thesis work, and how we might therapeutically take advantage of these pathways in a physiologic environment. Overall, this work suggests that the addition of Hsp70 inhibitors to current chemotherapeutic regiments would be highly effective and bypass common mechanisms of resistance.

5.2 Conclusions

A major goal of this thesis work was to clarify the role that Hsp70 plays in keeping cancer cells alive. Hsp70 was known to inhibit apoptosis (*1*, *2*) and it was thought to stabilize oncogenic client proteins, similar to Hsp90 (*3*–*5*). However, the full scope of Hsp70's functions in cancer was not clear. The central tenet of this thesis work is that tool compounds would provide new insight into these questions. In part, this approach is modeled after the long history of Hsp90 inhibitors. In 1994, Len Neckers and colleagues showed that geldanamycin destabilizes client kinases through inhibition of Hsp90 (*6*). This fortuitous discovery launched a concerted effort to develop increasingly more potent and selective Hsp90 inhibitors. Importantly, these efforts also provided chemical probes that revolutionized our understanding of Hsp90's pro-survival roles in cancer.

Unfortunately, Hsp70 has proven a much more difficult drug target. Hsp70 has a significantly higher affinity for nucleotide than Hsp90 (*7*), making it more difficult for active-site inhibitors to compete with endogenous nucleotide (*8*, *9*). Accordingly, a number of small molecules targeting other sites on Hsp70 have been developed, but have struggled with potency and selectivity (*10*–*13*). The difficulty of targeting the ATP-binding site of Hsp70 is also illustrated by the difficulty of finding small molecule fragments that bind this region – Hsp70 has one of the lowest "hit rates" of any target yet described (*7*).

When I joined the Gestwicki laboratory in 2011, Yoshinari Miyata and Xiaokai Li had just begun revisiting an abandoned Hsp70 inhibitor, MKT-077, as a possible alternative to ATP-competitive molecules. MKT-077 is a rhodacyanine that was

originally developed as a dye by Fuji Film Corp. This compound was found to have anti-cancer activity during unbiased screens of the Fuji Film chemical collection and MKT-077 was eventually advanced to clinical trials (*14*, *15*). It was later discovered that MKT-077 exerted its cytotoxicity through Hsp70, especially mtHsp70 and Hsc70 (*16*). Despite its promising activity, MKT-077 was abandoned in Phase I trials due to acquired nephrotoxicity (*17*), a result of labile metabolism and renal accumulation. However, our group noticed that MKT-077 was identified in a small group of analogs, without substantial medicinal chemistry efforts to optimize its properties. Further, its binding site wasn't known, precluding structure-guided design. In collaboration with Erik Zuiderweg's group, our lab showed that MKT-077 binds to a conserved, allosteric pocket on the NBD of Hsp70, leading to inhibition of its enzymatic functions (*18*). Further, Yoshinari Miyata, in collaboration with Duxin Sun's group (UM), identified the major metabolites of MKT-077 and its analogs (*19*). Together, these observations suggested ways of rationally improving the stability and potency of MKT-077 – and paving the way to making the first selective Hsp70 chemical probes.

In Chapter 2, I described the development of first generation derivatives of MKT-077 with increased potency and improved metabolic stability. We found that halogenation of the benzothiazole ring and replacement of the pyridine with a thiazole ring resulted in improved activity and half-life (Figure 5.1). Similar to MKT-077, the newer analogs seem to trap Hsp70 in an ADP-bound conformation. This state has a lower affinity for nucleotide exchange factor (NEF) co-chaperones (*20*) and seems to position client proteins for proteasomal degradation. Another graduate student in the group, Zapporah Young, is fully characterizing the molecular mechanisms of these

molecules and studying how the ADP-bound conformation is linked to enhanced client turnover. One interesting observation from these studies was that the MKT-077 analogs, such as JG-98, were not toxic to MEFs or normal cells, such as HepG2s. Why are these inhibitors so well tolerated when molecular chaperones constitute 2-5% of the cellular content? One possibility is that there are unique Hsp70 complexes that exist only in cancer cells and that are more sensitive to inhibitors, as has been suggested for Hsp90 (*21*). Our data shows that JG-98 reduces the ability of Hsp70 to interact with its co-chaperones, consistent with this idea. Another possibility is that normal cells have reduced protein turnover and a surplus of proteostasis capacity, such that if a portion of the Hsp70 is inhibited, the other chaperones can compensate. Cancer cells, on the other hand, express numerous mutated proteins that are prone to degradation. Increased chaperone activity is required to prevent turnover of these oncogenic drivers. Furthermore, rapid cellular division and exposure to conditions like ischemia, acidity, and oxidation result in a constitutively activated stress response. In these cells, a loss of Hsp70 function causes catastrophic proteostatic collapse. Another student in the group has recently completed a SILAC mass spectrometry experiment that will begin to address these possibilities (see Future Work below).

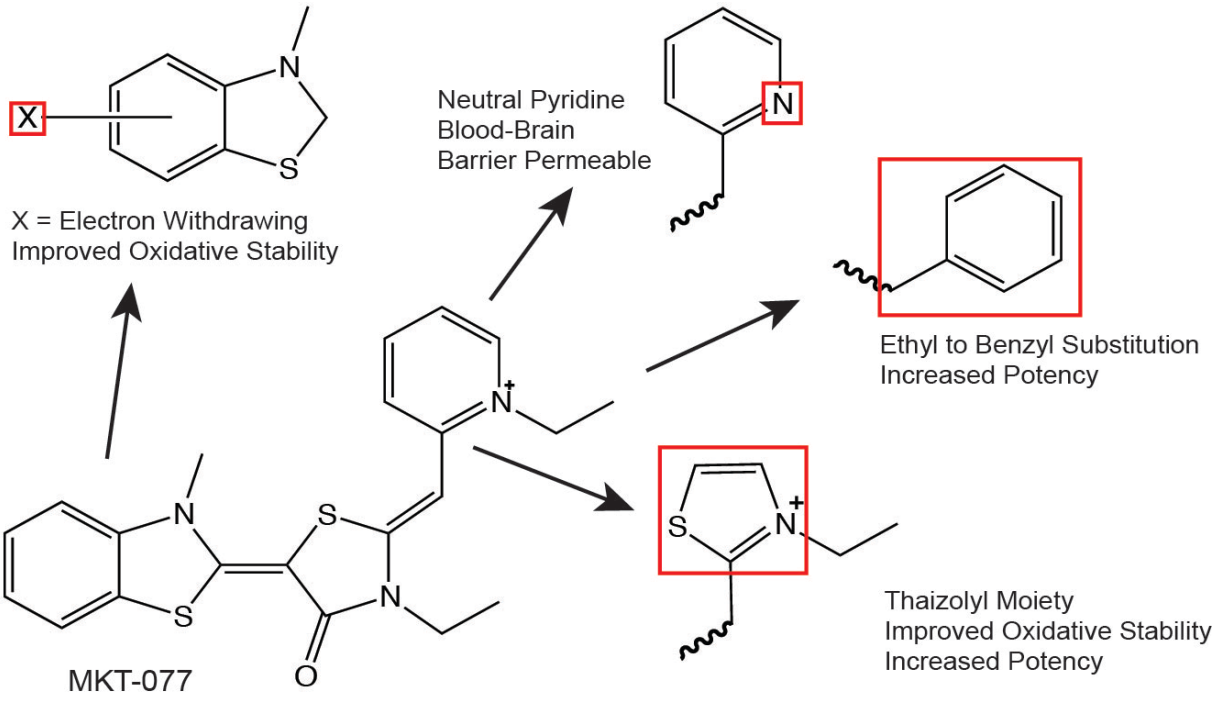

Figure 5.1 Improvements to the MKT-077 Scaffold. Various chemical modulations to the rhodocyanine scaffold have increased the metabolic stability and cell peremeability of MKT-077, as well as improving its potency.

The result of the studies in Chapter 2 was JG-98, a selective and relatively potent (EC_{50} ~ 400 nM) inhibitor of Hsp70. In Chapter 3, I used this new reagent to probe the roles of Hsp70 in cancer. Consistent with earlier hypotheses, JG-98 treatment induced modest degradation of Hsp90 clients. However, the kinetics of cytotoxicity did not match the rate of protein loss, as it does with Hsp90 inhibitors. Instead, JG-98 activated a RIP1-dependent pathway by coordinating degradation of the IAPs and cFLIP proteins. This RIP1 process appears to be novel as cytotoxicity was independent of TNF-R signaling, and no complex of RIP1 and Caspase-8 could be detected after compound treatment. However, JG-98 was still able to exploit RIP1's unique capacity to facilitate both apoptosis and, when combined with a caspase inhibitor, necroptosis. In addition,

we found that JG-98 could engage the mitochondrial death pathway independent of Bcl-2 status, the first compound ever to do so. Together, these studies provide new insights into the surprisingly broad roles played by Hsp70 in cancer. We anticipate that these studies are only the beginning of efforts to understand Hsp70 functions (see Future Studies below).

Another goal of my thesis work was to define the roles assigned to individual Hsp70 isoforms, especially in regards to the survival of cancer cells. The cationic MKT-077 analogs, including JG-98, localize largely to the mitochondria and, based on shRNA screens, are sensitive to the levels of mtHsp70/mortalin. Mitochondrial localization of MKT-077 analogs is likely to be particularly strong in cancer cells (*22*, *23*). However, the binding site on Hsp70 is universally conserved amongst human isoforms, and MKT-077 was able to pull down both mtHsp70 and cytosolic Hsc70. Further, JG-98 perturbs cytosolic clients. Together, these findings suggest that the charged analogs of MKT-077, act through both mortalin and the cytosolic Hsp70s.

In Chapter 4, we discuss the development of JG-13, a neutral derivative of MKT-077. To develop JG-13, we removed the cation from MKT-077, hypothesizing that this change would disfavor accumulation in the mitochondria. Concordant with this, in collaboration with Jonathan Weissman's Lab at UCSF, we found that JG-13 predominately relies on cytosolic Hsp70s for its cytotoxicity. Thus, this probe appears to be the first step towards chemical probes that can distinguish between Hsp70 isoforms. Moreover, the Gestwicki lab has previously shown that neutral derivatives of MKT-077 do not accumulate in the kidney and even penetrate the blood-brain barrier (*19*). Thus,

compounds such as JG-13 also have potential applications for treating neurological malignancies.

Interestingly, JG-13 had a very different cytotoxicity profile than JG-98. Although both compounds elicited cell death with similar kinetics and appeared to trigger apoptotic features by flow cytometry, JG-13 had a number of unique features. Fluorescence microscopy showed a lack of membrane blebbing or nuclear fragmentation, and was instead characterized by discrete punctae and flattened cells, more consistent with autophagy. Further, JG-13 had little effect on Hsp90 clients such as Raf-1 or Akt. Thus, despite binding to a conserved pocket, and eliciting similar allosteric perturbations, JG-13 directs a cell death very distinct from other Hsp70 inhibitors.

The observations from experiments with JG-98 and JG-13 have significantly advanced our understanding of Hsp70's roles in protecting against cell death (Figure 5.2). However, they also reveal how much more we have to uncover about proteostasis in cancer. In the remainder of this chapter, I will discuss some future experiments to shed light on these questions. Finally, I will suggest how Hsp70 inhibitors might be incorporated into chemotherapeutic regiments.

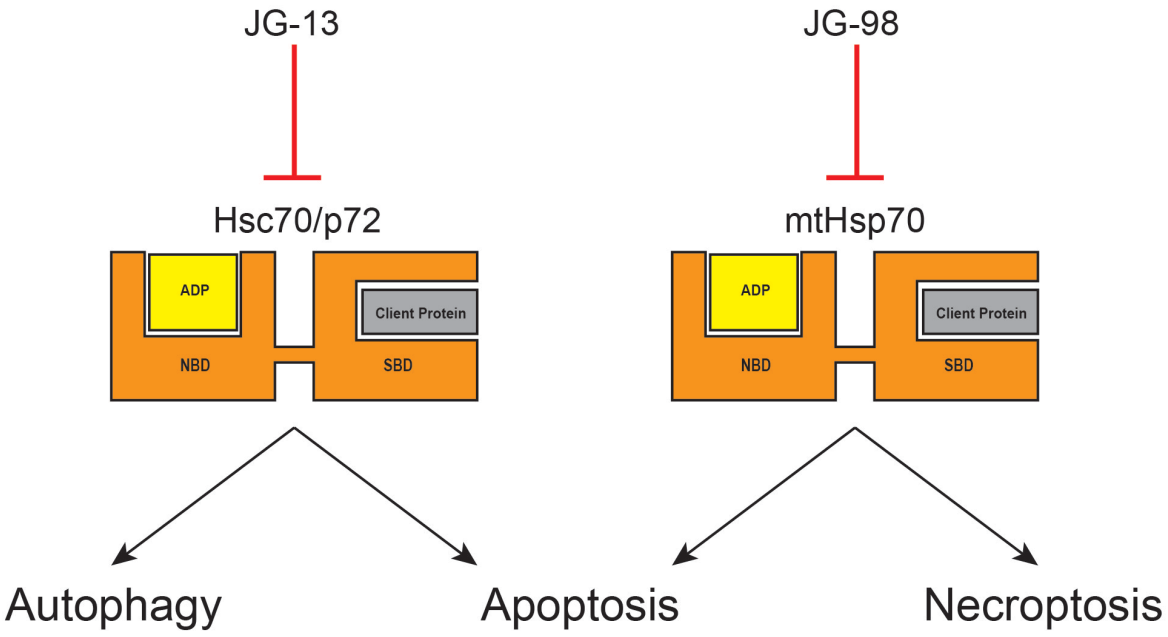

Figure 5.2 MKT-077 Analogs Trigger Multiple Cell Death Pathways. Targeted inhibition of cytosolic Hsp70 members by JG-13 appears to initiate features consistent with apoptosis and/or autophagy. Conversely, use of JG-98, and its effects on mtHsp70, can trigger either apoptotic or necroptotic pathways through RIP1.

5.3 Future Directions

5.3.1 Second Generation Derivatives of MKT-077 – Moving Beyond JG-98

The work in Chapter 2 showed that structure-guided design could result in the development of an analog of MKT-077 with superior stability and potency, JG-98. Using a combination of NMR (*24*) and Molecular Modeling (performed by Bryan Dunyak, a graduate student in the Gestwicki Lab), we've been able to model the conformational orientation of JG-98 as it binds to Hsp70. These structures have improved our understanding of JG-98's allosteric effects on the chaperone, and have suggested how even more potent analogs of JG-98 might be made. While not discussed in detail here, Xiaokai Li recently found that the new compounds have EC_{50} values of ~70 nM, which is 4-5 times more potent than JG-98. Further studies to examine the pharmacokinetic properties of these newer derivatives are warranted, as is mechanistic confirmation. However, it is clear that these allosteric inhibitors of Hsp70 can be modified to resemble more "drug-like" molecules. My thesis work will be an important guide in the development and optimization of these molecules. Specifically, activity in the RIP1 pathways can be used as an assay to guide development of the chemical series. Previous efforts (in other research groups) have largely focused on using the destabilization of Hsp90 clients as a primary endpoint for chemical optimization, a functional readout that appears to be less important for targeting Hsp70. Thus, the new insights provided by our work could provide an important advance.

5.3.2 Identification of Hsp70's Control on RIP1 Cytotoxicity

In Chapter 3, we determined that JG-98 activated a RIP1-dependent pathway that could activate both apoptosis and necroptosis. However, we still don't know how Hsp70 inhibition results in the activation of RIP1. Is Hsp70-mediated degradation of the IAPs sufficient to activate RIP1? Or is some other process involved? Does Hsp70 bind directly to RIP1 or the IAPs? An examination of the binding partners of RIP1 in response to JG-98 treatment might give insight into these questions. One potential experiment would be to immunoprecipitate RIP1 after JG-98 treatment, and assess its binding partners by mass spectrometry. Understanding the unique activation of RIP1's cytotoxic abilities will be important as we move towards pre-clinical advancement of these compounds.

5.3.3 Proteomic Analysis of Hsp70-Dependency

Another exciting use of the chemical tools, like JG-98 and JG-13, is to define the Hsp70-dependent proteome. Hsp90 inhibitors have helped define the "Hsp90-ome", to consist of approximately 200 kinases, transcription factors and oncogenes (*25*–*27*). However, similar studies have not been performed with Hsp70 due to the lack of chemical probes. Another student in the Gestwicki Lab, Laura Cesa, has recently started to use JG-98 in combination with SILAC, a powerful mass spectrometry platform, to help define the "Hsp70-ome" (Figures 5.3.A and B). It will be interesting to see if the proteomic changes observed with JG-98 can provide mechanistic insight into how apoptotic or necroptotic pathways are activated (Figures 5.3.C and D). In addition, comparing the profiles seen with JG-98 versus JG-13 may also allow the definition of

isoform-specific proteomes and further clarify functional distinctions of Hsp70 family members.

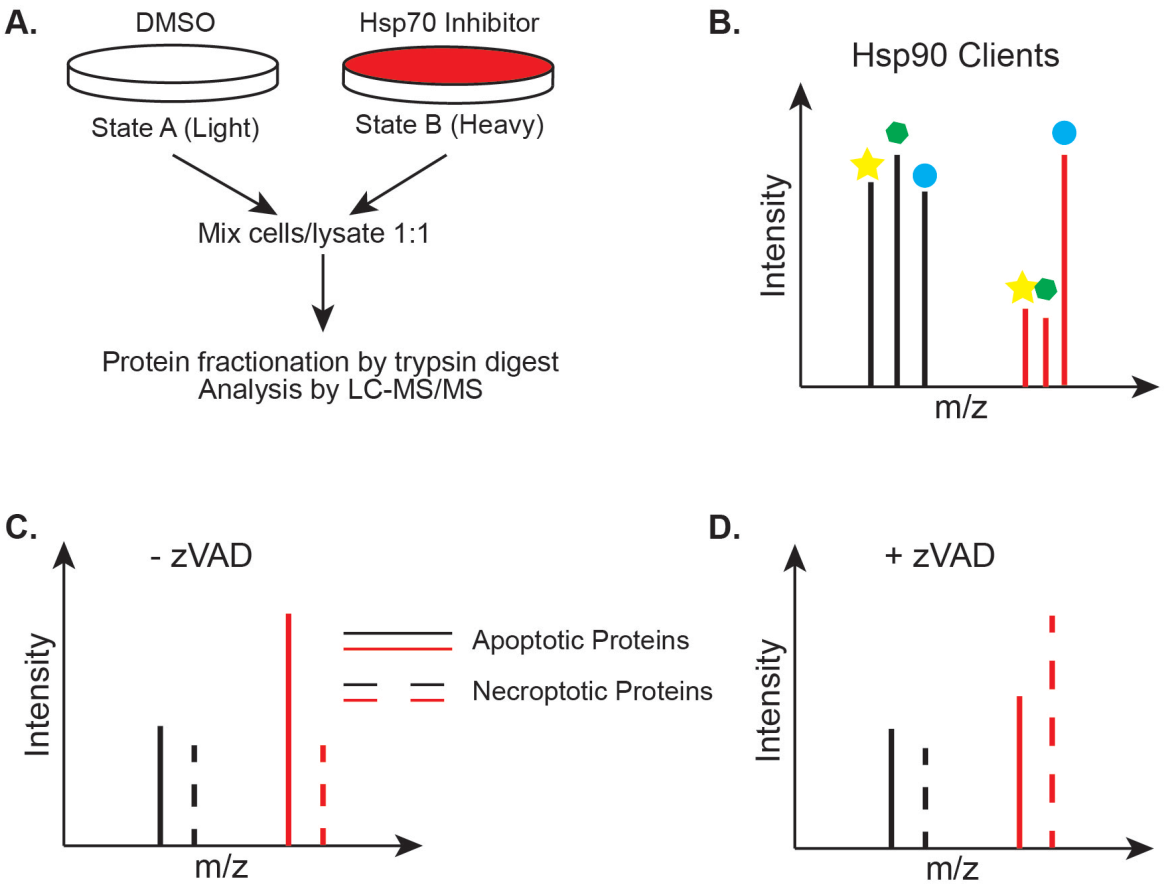

Figure 5.3 Mass Spectrometry Tools to Reveal Hsp70-Dependent Proteome. **(A)** Basic schematic: cells are labeled with heavy amino acids (Arg and Lys), and then treated with an Hsp70 inhibitor. Lysates are mixed, digested, and then analyzed by LC-MS/MS. **(B)** One important subset will be to analyze Hsp90 clients. Based on this thesis work, Hsp70 likely operates on some, but not all Hsp90 clients. Using this technology, we can get an unbiased profile of the apoptotic **(C)**, or necroptotic pathways **(D)** activated by Hsp70 inhibition.

5.3.4 Understanding the True Driving Factors of Cancer, Examination of Chaperones as Facilitators of Oncogenesis

One caveat of oncogenesis is that mutations in different proteins can lead to cancer, and that tumor specificity is often determined by the initial insult. For example, over 95% of pancreatic cancers are driven by a mutation in the oncogene Kras (*28*, *29*). Thus, with regards to this thesis work, one question is whether different cell lines, driven by different mutations, would respond similarly to an Hsp70 inhibitor like JG-98. For example, if JG-98 was cytotoxic to a Kras-mutated cell line, would the toxicity proceed through loss of Kras? Or some other independent pathway? That is, would a mutated Kras still be under the control of Hsp70, and thus degraded in response to inhibition with JG-98? Studies like the SILAC experiment proposed above will help our understanding of Hsp70's regulation of different oncogenes, and the extent to which they are dependent. It is possible that JG-98 will exert differential effects on cell lines with unique driver mutations.

However, at this point it is also worth returning to the argument made for the importance of chaperones in cancer. The same mutations, like in Kras, that promote unchecked proliferation or evasion of cell death, also render the protein unstable and prone to degradation. Without the upregulated activation of chaperone activity beforehand, these proteins would be discarded before oncogenesis could occur. Thus, it is possible to consider *increased chaperone function* as the initial insult to drive oncogenic activity, a theory that has been previously suggested (*25*, *30*). In this context, the cytotoxic potential of a chaperone inhibitor, like JG-98, would not be altered by

unique driver mutations, but rather by differential activation of the protein quality machinery.

5.3.5 Progress Towards the Clinic – Studying the Effects of Hsp70 Inhibitors *in vivo*

The work presented in this thesis has enormous therapeutic implications. However, in order to advance to clinical scenarios, it is important to study the effects of these compounds *in vivo* to understand the physiological realities of Hsp70 inhibition. To this end, we have collaborated with Michael Sherman (Boston University) and Byron Hann (UCSF) to study the effects of MKT-077 analogs in mouse models. In dose escalation studies, we found that JG-98 was well tolerated at 3mg/kg given i.p. twice weekly. We did not observe any evidence of renal damage or other toxicity in these animals and the compound lifetime was calculated to be ~10 hrs. In addition, preliminary xenografts of MCF-7 cells have been conducted, using the earlier analog YM-01 (Figure 5.4). The results suggest that MKT-077 analogs have efficacy *in vivo*, preventing tumor growth over long periods of time. Work is also underway to analyze the effects of newer derivatives, including JG-98 and JG-13, in the same xenograft models. In these planned studies, we are particularly interested in whether the more potent molecules reduce tumor volumes, instead of preventing growth as YM-01 does.

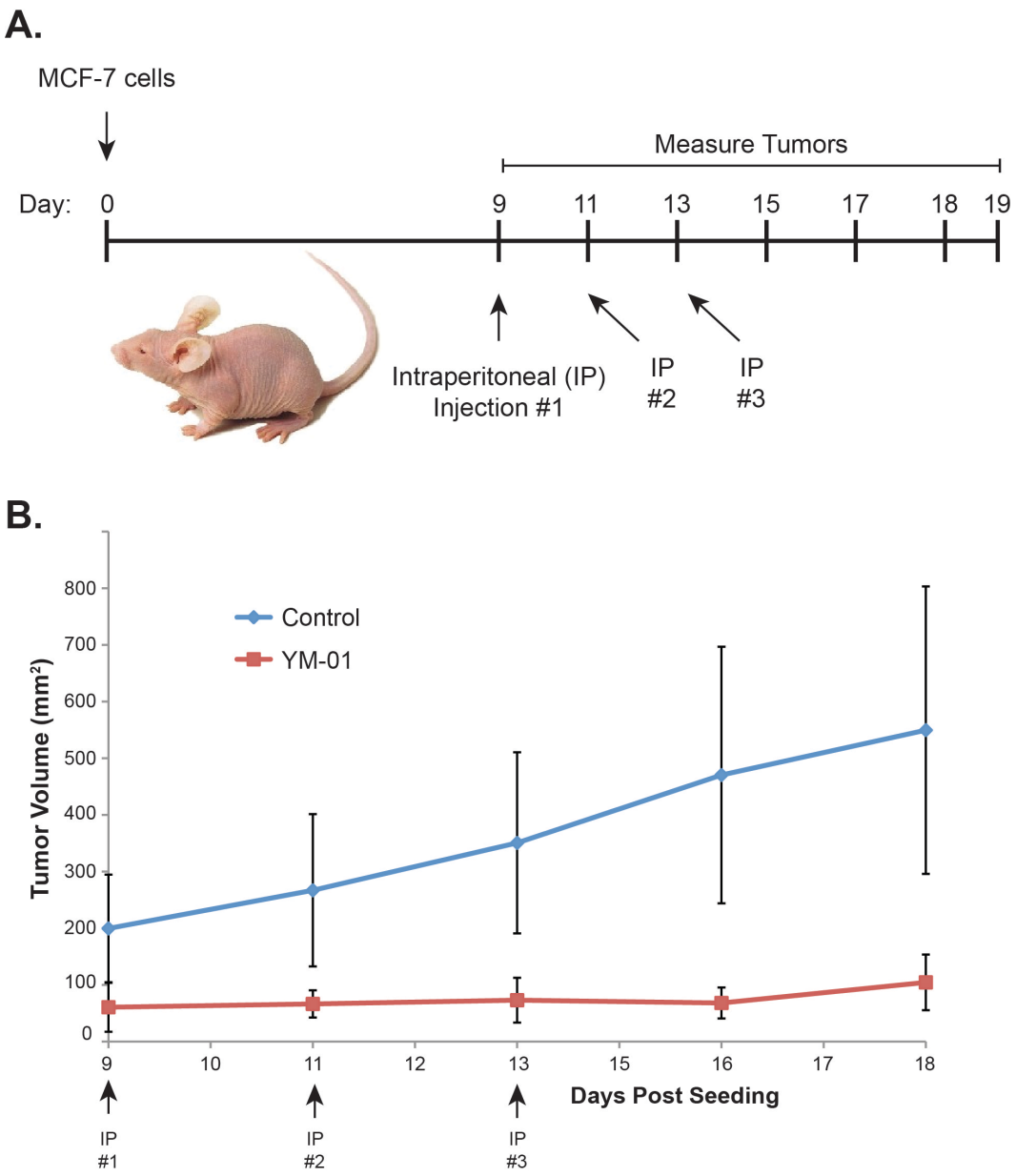

Figure 5.4 MKT-077 Analogs Have Activity *in vivo*. (A) Xenograft experimental design: 1 x 106 MCF-7 cells were subcutaneously injected into the right and left flanks of 6 mice (12 tumors total). IP injections of YM-01 (0.5mg/mouse in DMSO, diluted in PBS) were administered at 9, 11, and 13 days post-seeding. **(B)** Comparative growth of treated vs control (DMSO in PBS) tumors. YM-01 treated samples display significantly delayed growth. Figure provided from Sherman Lab (Boston U.)

The results of Chapter 3 also suggest that JG-98 might be used to treat malignancies where the mitochondrial death pathway has been inactivated. Specifically, these studies showed that JG-98 triggered cytochrome c release independent of Bcl-2 status. This mechanism could be important in follicular lymphoma, which is driven by a translocation that increases the levels of Bcl-2 members (*31*). This cancer currently lacks any truly effective therapies and is regarded as incurable. Thus, pre-clinical studies of lymphoma models using JG-98 as part of the treatment regimen are an exciting future application.

We are also excited to test JG-98 and its analogs in mice with a humanized immune system. Recently, nod *scid* gamma (NSG) mice have been shown to acquire bone marrow grafts that completely recapitulate the human immune system (reviewed in (*32*)). This model would allow us to study not only tolerance of MKT-077 analogs in a more physiological setting, but also their efficacy. It has previously been shown that Hsp70 works in conjunction with immune regulators (*33*, *34*), and that inhibitors can be potentiated by the presence of a working immune system (*35*). Thus, it is possible that JG-98's effects *in vivo* might be more dramatic combined with the existing cytotoxic functions in these mice models.

Lastly, the ability of JG-98 to kill apoptosis-resistant cells begs the question of the physiological relevance of necroptosis. Would a cancer that was completely resistant to apoptosis (e.g. deprived of all caspases), undergo necroptosis when treated with JG-98? Would a mouse model of this cancer show inflammation? The use of the models described above, along with newer genetic tools such as TALENS or CRISPR/Cas9 to disrupt endogenous gene function may help answer these questions.

5.4 Final Thoughts

The work presented herein has made significant progress towards understanding the roles Hsp70 plays in maintaining the cancer phenotype. I was also able to advance our knowledge of how Hsp70 might be exploited as a cancer drug target. The most important finding was that Hsp70 guards against multiple cell death pathways, and operates quite differently from other members of the protein quality control machinery. Also this thesis work definitively answers speculations on synergistic activity of an Hsp70 inhibitor with compounds targeting Hsp90 or the proteasome, and makes headway towards selectively inhibiting individual members of the Hsp70 family. Together, this work argues not only for the implementation of Hsp70 inhibitors in clinical settings, but also for their use as probes to understand regulation of proteostasis in cancer cells. It will be important to examine multiple cancer models, both *in cellulo* and *in vivo*, as the principles uncovered here are not likely to be universal. Moving forward, unbiased, interdisciplinary studies driven by collaborations will reveal more intricacies about the oncogenic function of Hsp70, and better position us for successful therapeutic intervention.

5.5 References

1. A. Saleh, S. M. Srinivasula, L. Balkir, P. D. Robbins, E. S. Alnemri, Negative regulation of the Apaf-1 apoptosome by Hsp70, *Nat Cell Biol* **2**, 476–483 (2000).
2. A. R. Stankiewicz, G. Lachapelle, C. P. Foo, S. M. Radicioni, D. D. Mosser, Hsp70 inhibits heat-induced apoptosis upstream of mitochondria by preventing Bax translocation, *J Biol Chem* **280**, 38729–38739 (2005).
3. M. V Powers, P. A. Clarke, P. Workman, Dual targeting of HSC70 and HSP72 inhibits HSP90 function and induces tumor-specific apoptosis, *Cancer Cell* **14**, 250–262 (2008).
4. E. L. Davenport *et al.*, Targeting heat shock protein 72 enhances Hsp90 inhibitor-induced apoptosis in myeloma, *Leukemia* **24**, 1804–1807 (2010).
5. D. S. Williamson *et al.*, Novel adenosine-derived inhibitors of 70 kDa heat shock protein, discovered through structure-based design, *J Med Chem* **52**, 1510–1513 (2009).
6. L. Whitesell, E. G. Mimnaugh, B. De Costa, C. E. Myers, L. M. Neckers, Inhibition of heat shock protein HSP90-pp60v-src heteroprotein complex formation by benzoquinone ansamycins: essential role for stress proteins in oncogenic transformation., *Proc. Natl. Acad. Sci.* **91**, 8324–8328 (1994).
7. A. J. Massey, ATPases as drug targets: insights from heat shock proteins 70 and 90, *J Med Chem* **53**, 7280–7286 (2010).
8. A. J. Massey *et al.*, A novel, small molecule inhibitor of Hsc70/Hsp70 potentiates Hsp90 inhibitor induced apoptosis in HCT116 colon carcinoma cells, *Cancer Chemother Pharmacol* **66**, 535–545 (2010).
9. H. J. Cho *et al.*, A small molecule that binds to an ATPase domain of Hsc70 promotes membrane trafficking of mutant cystic fibrosis transmembrane conductance regulator, *J Am Chem Soc* **133**, 20267–20276 (2011).
10. J. I. Leu, J. Pimkina, A. Frank, M. E. Murphy, D. L. George, A small molecule inhibitor of inducible heat shock protein 70, *Mol Cell* **36**, 15–27 (2009).
11. E. Schmitt, A. Parcellier, S. Gurbuxani, Chemosensitization by a Non-apoptogenic Heat Shock Protein 70-Binding Apoptosis-Inducing Factor Mutant, *Cancer Res.* , 8233–8240 (2003).
12. M. J. Braunstein *et al.*, Antimyeloma Effects of the Heat Shock Protein 70 Molecular Chaperone Inhibitor MAL3-101, *J Oncol* **2011**, 232037 (2011).
13. K. A. Havlin *et al.*, Deoxyspergualin: phase I clinical, immunologic and pharmacokinetic study, *Anticancer Drugs* **6**, 229–236 (1995).
14. Y. Chiba *et al.*, MKT-077, localized lipophilic cation: antitumor activity against human tumor xenografts serially transplanted into nude mice, *Anticancer Res* **18**, 1047–1052 (1998).
15. K. Koya *et al.*, MKT-077, a novel rhodacyanine dye in clinical trials, exhibits anticarcinoma activity in preclinical studies based on selective mitochondrial accumulation, *Cancer Res* **56**, 538–543 (1996).
16. R. Wadhwa, T. Sugihara, A. Yoshida, H. Maruta, S. C. Kaul, Selective Toxicity of MKT-077 to Cancer Cells Is Mediated by Its Binding to the hsp70 Family Protein mot-2 and Reactivation of p53 Function Advances in Brief Selective Toxicity of

MKT-077 to Cancer Cells Is Mediated by Its Binding to the hsp70 Family Prot, , 6818–6821 (2000).
17. C. Britten, E. Rowinsky, S. Baker, A phase I and pharmacokinetic study of the mitochondrial-specific rhodacyanine dye analog MKT 077, *Clin. cancer …* , 42–49 (2000).
18. A. Rousaki *et al.*, Allosteric drugs: the interaction of antitumor compound MKT-077 with human Hsp70 chaperones, *J Mol Biol* **411**, 614–632 (2011).
19. Y. Miyata *et al.*, Synthesis and Initial Evaluation of YM-08, a Blood-Brain Barrier Permeable Derivative of the Heat Shock Protein 70 (Hsp70) Inhibitor MKT-077, Which Reduces Tau Levels., *ACS Chem. Neurosci.* , 8–10 (2013).
20. J. N. Rauch, J. E. Gestwicki, Binding of human nucleotide exchange factors to heat shock protein 70 (hsp70) generates functionally distinct complexes in vitro., *J. Biol. Chem.* **289**, 1402–14 (2014).
21. A. Kamal *et al.*, A high-affinity conformation of Hsp90 confers tumour selectivity on Hsp90 inhibitors, *Nature* **425**, 407–410 (2003).
22. B. G. Heerdt, M. A. Houston, L. H. Augenlicht, The intrinsic mitochondrial membrane potential of colonic carcinoma cells is linked to the probability of tumor progression., *Cancer Res.* **65**, 9861–7 (2005).
23. M. R. Duchen, Contributions of mitochondria to animal physiology: from homeostatic sensor to calcium signalling and cell death, *J. Physiol.* **516**, 1–17 (1999).
24. X. Li *et al.*, Analogues of the Allosteric Heat Shock Protein 70 (Hsp70) Inhibitor, MKT-077, As Anti-Cancer Agents, *ACS Med Chem Lett* **70** (2013).
25. M. Taipale *et al.*, Quantitative analysis of HSP90-client interactions reveals principles of substrate recognition, *Cell* **150**, 987–1001 (2012).
26. R. S. Samant, P. A. Clarke, P. Workman, The expanding proteome of the molecular chaperone HSP90, *Cell Cycle* **11**, 1301–1308 (2012).
27. V. C. H. da Silva, C. H. I. Ramos, The network interaction of the human cytosolic 90 kDa heat shock protein Hsp90: A target for cancer therapeutics., *J. Proteomics* **75**, 2790–802 (2012).
28. S. Jones *et al.*, Core signaling pathways in human pancreatic cancers revealed by global genomic analyses., *Science* **321**, 1801–6 (2008).
29. R. H. Hruban *et al.*, Pancreatic intraepithelial neoplasia: a new nomenclature and classification system for pancreatic duct lesions., *Am. J. Surg. Pathol.* **25**, 579–86 (2001).
30. S. L. Rutherford, S. Lindquist, Hsp90 as a capacitor for morphological evolution., *Nature* **396**, 336–42 (1998).
31. D. E. Horsman, R. D. Gascoyne, R. W. Coupland, A. J. Coldman, S. A. Adomat, Comparison of cytogenetic analysis, southern analysis, and polymerase chain reaction for the detection of t(14; 18) in follicular lymphoma., *Am. J. Clin. Pathol.* **103**, 472–478 (1995).
32. L. D. Shultz, M. A. Brehm, J. V. Garcia-Martinez, D. L. Greiner, Humanized mice for immune system investigation: progress, promise and challenges., *Nat. Rev. Immunol.* **12**, 786–98 (2012).
33. K. Juhász *et al.*, Lysosomal rerouting of Hsp70 trafficking as a potential immune activating tool for targeting melanoma., *Curr. Pharm. Des.* **19**, 430–40 (2013).

34. P. Stocki, X. N. Wang, A. M. Dickinson, Inducible heat shock protein 70 reduces T cell responses and stimulatory capacity of monocyte-derived dendritic cells., *J. Biol. Chem.* **287**, 12387–94 (2012).
35. E. Schmitt *et al.*, Heat shock protein 70 neutralization exerts potent antitumor effects in animal models of colon cancer and melanoma, *Cancer Res* **66**, 4191–4197 (2006).